

HIGH-SPEED IMAGING OF POLYMER INDUCED FIBER FLOCCULATION

A Thesis
Presented to
The Academic Faculty

by

William H. Hartley

In Partial Fulfillment
of the Requirements for the Degree
Master of Science in the
School of Chemical and Biomolecular Engineering

Georgia Institute of Technology

May 2007

HIGH-SPEED IMAGING OF POLYMER INDUCED FIBER FLOCCULATION

Approved by:

Dr. Sujit Banerjee, Advisor
School of Chemical and Biomolecular Engineering
Georgia Institute of Technology

Dr. Jim Frederick
School of Chemical and Biomolecular Engineering
Georgia Institute of Technology

Dr. Tim Patterson
School of Mechanical Engineering
Georgia Institute of Technology

Date Approved: February 28, 2007

To my fiancé,

Annie,

who always offers her love, devotion, and support no matter what.

ACKNOWLEDGEMENTS

I would like to thank my advisor Sujit Banerjee for allowing me to join his group and providing the opportunity to pursue a Masters degree without too much grief. Also, I appreciate his patience due to the limited knowledge base of the pulp and paper industry I had before this project. Kiran, Fran, Rob, and Brett also deserve credit, as they explained answers to my questions regardless of the triviality of the inquiries.

My family has always offered support to all my decisions, and as such, deserve thanks as well. I thank my father for never allowing me to quit anything I started and for his motivational speeches. I give thanks also to my mother for listening and supporting me through all of the tough times and my sister for always being there for me and the reminders that “there is light at the end of the tunnel.”

Finally and most importantly, I would like to thank my fiancé, Annie. No matter how difficult my day, she is always able to elevate my mood. She is consistently there for me, and I could not have accomplished this project without her love and support.

TABLE OF CONTENTS

	Page
ACKNOWLEDGEMENTS	iv
LIST OF TABLES	vii
LIST OF FIGURES	viii
SUMMARY	x
<u>CHAPTER</u>	
1 INTRODUCTION	1
2 LITERATURE REVIEW	2
2.1 Fiber Properties	2
2.2 Fiber Fines	4
2.3 Hydrogen Bonding	4
2.4 Floc Structure	5
2.4.1 Factors Affecting Floc Structure	5
2.5 Polymer Adsorption	6
2.5.1 Charge Neutralization	7
2.5.2 Bridging	7
2.5.3 Patching	9
2.5.4 Complex Flocculation	10
2.6 Flocculation Kinetics	10
2.6.1 Techniques for Measuring Flocculation Kinetics	11
2.6.2 Reporting Flocculation Kinetics	11
2.6.3 Results of Flocculation Kinetics	12
3 EXPERIMENTAL	13

3.1	Fiber and Polymer Preparation	13
3.1.1	Short and Long Fiber Separation	13
3.1.2	Fiber Quality Analyzer (FQA)	14
3.1.3	Cationic Polyacrylamide (cPAM) Preparation	15
3.2	Procedure	15
3.3	Measurement Error	19
3.4	Replication	19
3.5	Materials	21
4	RESULTS AND DISCUSSION	22
4.1	Long Fiber (2/3) and Short Fiber (1/3)	22
4.2	Long Fiber (1/3) and Short Fiber (2/3)	28
4.3	All Long Fiber	34
4.4	Unfractionated Fiber	40
4.5	Comparison of Different Fiber Amounts	45
4.6	cPAM Isotherm	47
4.7	Effects of a Different Polymer	48
4.8	Effects of Shear Rate	49
4.9	Fiber Length	50
4.10	Fiber Floc Characterization	52
5	CONCLUSIONS/SUMMARY	53
	REFERENCES	56

LIST OF TABLES

	Page
Table 1: Amount of fiber present at the beginning and conclusion of a trial at 181 RPM and 2 ppm cPAM	17
Table 2: All of the trials performed	18
Table 3: Different trials performed for 2/3 long and 1/3 short fiber	23
Table 4: The starting and final avg. fiber lengths as a function of polymer concentration (2/3 long and 1/3 short)	28
Table 5: Different trials performed for 1/3 long and 2/3 short fiber	29
Table 6: The starting and final avg. fiber lengths as a function of polymer concentration (1/3 long and 2/3 short)	34
Table 7: Different trials performed for all long fiber	35
Table 8: The starting and final avg. fiber lengths as a function of polymer concentration (all long)	40
Table 9: Different trials performed for unfractionated fiber	41
Table 10: The starting and final avg. fiber lengths as a function of polymer concentration	45
Table 11: Comparison of results for the Eka and Hercules polymers	49
Table 12: Starting average fiber length and final average fiber length	54

LIST OF FIGURES

	Page
Figure 1: Softwood tracheid	3
Figure 2: Example of loops and tails	8
Figure 3: Adsorption of a bridging polymer	8
Figure 4: Bridging polymer during flocculation	9
Figure 5: Patch mechanism	9
Figure 6: Long fiber length distribution (Screen size 12)	14
Figure 7: Short fiber length distribution (Screen size 60)	14
Figure 8: Beginning (Time = 0 sec)	16
Figure 9: Middle (Time = 13 sec)	16
Figure 10: End (Time = 24 sec)	16
Figure 11: Graph of 3 trials of unfractionated fiber at 181 RPM and 2 ppm cPAM	19
Figure 12: Graph of 1/3 long and 2/3 short fiber at 181 RPM and 2 ppm cPAM	20
Figure 13: Graph of 2/3 long and 1/3 short fiber at 181 RPM and 2 ppm cPAM	20
Figure 14: Graph of all long fiber at 181 RPM and 2 ppm cPAM	21
Figure 15: Graph of 2/3 long and 1/3 short fiber, 2 ppm cPAM, and varying motor speeds of 100 RPM, 181 RPM, and 250 RPM	24
Figure 16: Graph of 2/3 long and 1/3 short fiber, 4 ppm cPAM, and varying motor speeds of 100 RPM, 181 RPM, and 250 RPM	25
Figure 17: Graph of 2/3 long fiber at cPAM concentrations of 0.1, 0.2, 1, 2, and 4 ppm at a motor speed of 181 RPM	27
Figure 18: Graph of 1/3 long and 2/3 short fiber, 2 ppm cPAM, and varying motor speeds of 100 RPM, 181 RPM, and 250 RPM	30

Figure 19:	Graph of 1/3 Long and 2/3 short fiber, 4 ppm cPAM, and varying motor speeds of 100 RPM, 181 RPM, and 250 RPM	31
Figure 20:	Graph of 1/3 long fiber at cPAM concentrations of 0.1, 0.2, 1, 2, and 4 ppm at a motor speed of 181 RPM	33
Figure 21:	Graph of all long fiber, 2 ppm cPAM, and varying motor speeds of 100 RPM, 181 RPM, and 250 RPM	36
Figure 22:	Graph of all long fiber, 4 ppm cPAM, and varying motor speeds of 100 RPM, 181 RPM, and 250 RPM	38
Figure 23:	Graph of all long fiber at cPAM concentrations of 0.1, 0.2, 1, 2, and 4 ppm at a motor speed of 181 RPM	39
Figure 24:	Graph of unfractionated fiber, 2 ppm cPAM, and varying motor speeds of 100 RPM, 181 RPM, and 250 RPM	42
Figure 25:	Graph of unfractionated fiber, 4 ppm cPAM, and varying motor speeds of 100 RPM, 181 RPM, and 250 RPM	43
Figure 26:	Graph of unfractionated fiber at cPAM concentrations of 0.1, 0.2, 1, 2, and 4 ppm at a motor speed of 181 RPM	44
Figure 27:	Graph of all long fiber, 2/3 long with 1/3 short, 1/3 long with 2/3 short, 100 RPM, and a cPAM concentration of 2 ppm	46
Figure 28:	Graph of all long fiber, 2/3 long with 1/3 short, 1/3 long with 2/3 short, 181 RPM, and a cPAM concentration of 2 ppm	46
Figure 29:	Graph of all long fiber, 2/3 long with 1/3 short, 1/3 long with 2/3 short, 250 RPM, and a cPAM concentration of 2 ppm	47
Figure 30:	cPAM isotherm at 181 RPM and various concentrations of polymer	48
Figure 31:	Graph of unfractionated fiber at 181 rpm and 2 ppm of Hercules DI373 and Eka 2610	49
Figure 32:	Difference in final and initial average fiber lengths with varying concentrations of cPAM.	52

SUMMARY

This study presents quantitative results on the effect on individual fiber length during fiber flocculation. Flocculation was induced by a cationic polyacrylamide (cPAM). A high speed camera recorded 25 second video clips. The videos were image-analyzed and the fiber length and the amount of fiber in each sample were measured. Prior to the flocculation process, fibers were fractionated into short and long fibers. Trials were conducted using the unfractionated fiber, short fiber, and long fiber. The short and long fibers were mixed in several trials to study the effect of fiber length. The concentration of cPAM was varied as well as the motor speed of the impeller (RPM). It was found that the average fiber length decreased more rapidly with increasing motor speed. Increasing the concentration of cPAM also led to a greater decrease in average fiber length. A key finding was that a plateau was reached where further increasing the amount of cPAM had no effect. Hence, fibers below a critical length resisted flocculation even if the chemical dose or shear was increased. This critical length was related to the initial length of the fiber.

CHAPTER 1

INTRODUCTION

Previous research has been conducted concerning the measurement of fiber floc formation. More specifically, there is quite a bit of work done on the imaging of fiber suspensions using a high-speed camera. This technique can provide images that when processed provide information about fiber flocs and individual fibers. Image analysis allows for the determination of the rate of floc formation, individual fiber length, floc area, and changes in average fiber length with time.

Fiber flocculation is induced by polymers such as cationic polyacrylamide (cPAM). Polymers are commonly used in the paper industry as retention aids. These retention aids serve to retain fiber fines and additives such as kaolin clay. Polymer induced floc formation is not just limited to the paper industry, but is also widely used in the wastewater industry. Sludge is usually conditioned with polymers, which leads to better dewatering.

Previous research does not quantify or illustrate how the length of individual fibers changes during the flocculation process. This study presents the effect of polymer induced flocculation and its effect on average fiber length reduction using a high-speed camera. Imaging can provide evidence that flocculation decreases the average fiber length of individual fibers not part of a floc. Variables in this investigation include: polymer concentration, fiber length, and impeller speed (RPM).

CHAPTER 2

LITERATURE REVIEW

2.1 Fiber Properties

Fibers are the main structural component of paper, and the type of fiber determines the paper properties. Several types of vascular wood and nonwood sources provide pulp fibers for the paper making industry [1, 2]. The properties of fibers are determined by several factors. Some of these factors include the type of wood, where the wood is harvested, and if it is chemically or mechanically pulped [3].

The structure of a softwood fiber contains several layers, and each layer has different properties. The three main layers are the middle lamella, the primary wall, and the secondary wall. The secondary wall consists of the S1, S2, and S3 layers. Within the secondary wall, the S1 layer is the outer coating, the S2 layer is the main structural component of the fiber, and the S3 layer is the inner layer next to the lumen [2, 3]. According to Eklund and Lindstrom, 80% of the wood fiber is from the S2 layer [1]. Lignin encompasses most of the middle lamella, while the primary wall consists of both microfibrils and lignin [1]. The softwood fiber is shown in Figure 1.

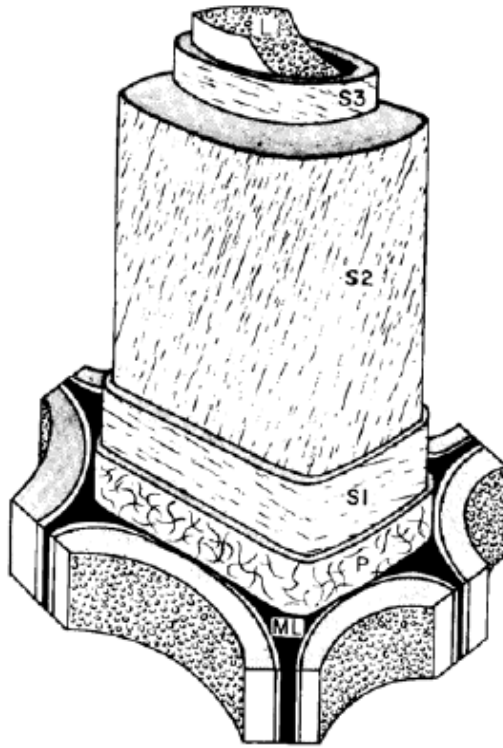


Figure 1: Softwood tracheid [2].

The fibers and cell wall layers consist of cellulose, hemicelluloses, and lignin. Cellulose is the reason fiber is used in papermaking. Cellulose contains carbon, oxygen, and hydrogen, which combined create a long-chain polymeric carbohydrate with a monomer building block of glucose [2, 4]. Hemicelluloses are also a polymeric material but are a shorter-chain polymeric carbohydrate than that of cellulose [4]. Hemicelluloses are comprised of multiple different sugars versus that of cellulose, which is made of only glucose [2, 4]. The pulping process determines the amount of cellulose that dissolves. Lignin is highly polymerized and is an amorphous material that holds the fibers together [2]. Fibers are delignified during the pulping process, which results in the removal of the middle lamella and the lignin from within the fiber walls [1].

2.2 Fiber Fines

In the papermaking furnish both fiber (of various lengths) and fines are present. Fines are defined in various ways but currently as parts of the fiber suspension that pass through a 200 mesh screen [5, 6]. Fines occur naturally or as the product of mechanical and chemical refining. Mechanical refining produces more fines than does chemical refining [3]. Fines present in pulp before refining are considered to be primary fines, and refining creates what is referred to as secondary fines [3, 4]. Compared to their parent fibers, fines have different properties [3]. Most importantly, there is a change in the specific surface area, which is defined as area per unit mass. According to Marton, fines have approximately 4-7 times larger specific surface area than that of their parent fibers [7]. This large surface area accounts for fines having increased swelling and absorption of more water than that of their parent fibers [3, 7]. Additionally, with a large specific surface area, additives in the furnish are more easily adsorbed and fiber to fiber bonding is increased [3, 4]. Fines add strength to the paper and can sometimes comprise up to 40% of the furnish weight [3, 4].

2.3 Hydrogen Bonding

Most aspects of papermaking occur in water, which is essential for the bonding of fibers. Fibers contain cellulose that readily absorbs water. Cellulose has an affinity for water and is hydrophilic in nature because of its ability to form hydrogen bonds [1]. Hydrogen bonding occurs between water molecules and other molecules that contain a hydroxyl functional group [4]. When the fibers undergo refining, they increase in size due to improved water absorption in the secondary cell wall [2]. Hydrogen bonding is enhanced by an increase in surface area from the refining action [2].

2.4 Flocculation Structure

Flocculation is the agglomeration of fibers and other particles suspended in a liquid medium. Several properties lead to the development of a floc and other aspects can destroy a floc. Mason explains that flocculation is dependent on certain fiber properties such as concentration, size, and shape [8]. An increase in pulp concentration corresponds to an increase in flocculation [9]. The size of the fiber plays an important role in agglomeration, because longer fibers result in a larger sized floc [10]. Also, it is known that shorter fibers tend to flocculate less, resulting in fewer flocs, when compared to longer fibers [11]. However, the rate of fiber length change during flocculation has not been studied or quantified. The two fundamental steps for floc formation are collision and adhesion [8]. A floc is created when fibers collide and attach to one another forming a base for growth, then this base is subjected to more collisions and continues to grow [8]. If a polymer is involved in the flocculation process, then polymer adsorption can be augmented by increased collisions [12].

2.4.1 Factors Affecting Flocculation Structure

Velocity and shear rate play a significant role in the collision process. The fibers can floc more effectively as a result of increasing the shear rate, which allows for more dynamic movement between fibers [13]. Adhesion describes the mechanism of fiber attachment. The two types of adhesion described by Mason are chemical flocculation and mechanical flocculation [8]. Chemical flocculation is affected by retention aids and adhesive coatings, whereas mechanical flocculation is heavily influenced by fiber physical properties such as splits, fibrillation, and surface roughness [8].

Kerekes [14] further categorizes the adhesion mechanism into four different categories which are colloidal, mechanical surface linkage, elastic fiber bending, and surface tension. The colloidal process is described by electrostatic forces between two fibers [14]. When a bent fiber cannot straighten out due to the amount of contact between itself and surrounding fibers, this force is referred to as elastic fiber bending [14]. Surface tension is involved when bubbles of gas are present and attract hydrophobic particulates resulting in agglomeration [14]. Floc breakup can occur by altering the same variables that allow flocs to be created. Some of these variables are temperature, velocity, and shear rate. It is known that a high shear rate increases floc formation, but continually increasing the rate eventually adds too much force and will destroy the floc [13]. Temperature also affects floc formation and breakup. A lower temperature corresponds with a reduction in floc size [15]. This is explained by an increase in viscosity which reduces turbulence, or a reduction in fiber to fiber approach velocity [15]. Also, since viscous forces dominate over inertial this leads to less fiber collisions [15]. Flocs can be classified as two different types, hard flocs and soft flocs. Hard flocs are usually induced by a cationic polymer and resist breaking up unless introduced to high shear rates [16]. Soft flocs at low shear levels can develop better fines retention and reagglomerate after periods of high shear [16].

2.5 Polymer Adsorption

Polymer usage in the paper industry plays a significant role in fiber flocculation. Different types of polymers can be employed based on the characteristics of the fiber suspension to which they are being added. Polymers can aid in the flocculation of not

only fibers but other components added to the furnish such as fillers. Retention aids cause fines to attach to the fiber mat, thus retaining the fines [1].

Several different mechanisms for polymer induced flocculation exist, and understanding each one is important in determining which retention aid to use. The different mechanisms include charge neutralization, hetero-coagulation, patching, bridging, complex flocculation, and network flocculation [1, 4].

2.5.1 Charge Neutralization

Charge neutralization involves adjusting the charge so the fibers and fines no longer repel each other but attract one another [17]. Flocculation by charge neutralization obeys DLVO-theory, which describes the reduction of the energy barrier, responsible for repulsion, by compression of the electrostatic double layer [1]. The number of counterions increases upon addition of an electrolyte to the solution, which reduces the charge difference. When the charge difference is significantly reduced and approaching zero, then flocculation will occur [4]. Flocs can be broken up if too much of the electrolyte is added [17]. An example of a charge neutralizing polymer would be one that is highly cationic with a low molecular weight [17].

2.5.2 Bridging

Bridging is another mechanism that is involved with fiber flocculation. First, the bridging mechanism involves the polymer adsorbing to the fiber [1, 17]. After the polymer is adsorbed it then extends out into solution and acts as a bridge as it attaches to oppositely charged particles and fibers [1]. Since the polymer can extend beyond the electrical double layer it increases the possible area for flocs to form [17]. Bridging polymers have loops and tails that form the bridges between fibers and other particulates

due to the surface interactions [17]. This is shown in Figure 2. The increased number of collisions between fibers reflects the effectiveness of bridging flocculation [4]. The type of polymer best suited for bridging flocculation would be one of high molecular weight, which has longer polymer chains [4, 17]. Figure 3 shows the initial adsorption of the polymer and Figure 4 shows the flocculation occurring.



Figure 2: Example of loops and tails [17].

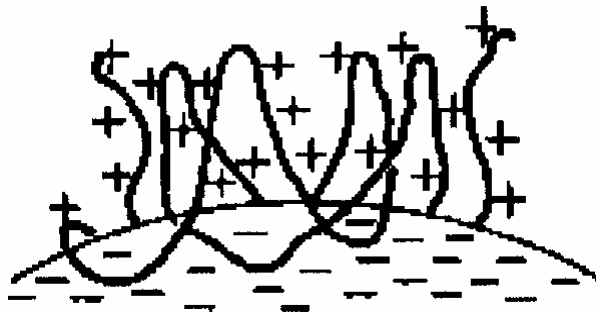


Figure 3: Adsorption of a bridging polymer [1].

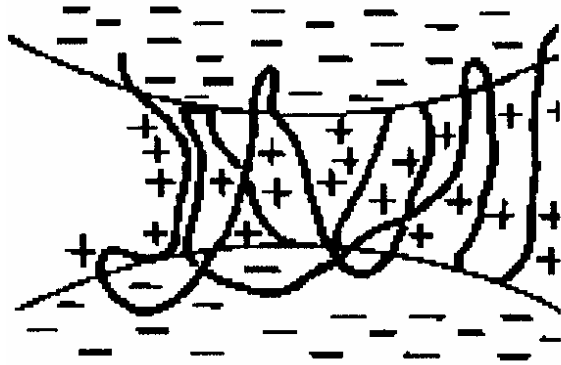


Figure 4: Bridging polymer during flocculation [1].

2.5.3 Patching

A third type of flocculation mechanism is that of the patch model. The patch mechanism involves a cationic polymer adsorbing onto the negatively charged surface of a fiber to create sites of positive charge [1, 4]. The rest of the fiber will remain anionic except for the sites of the deposited polymer [4]. This is shown in Figure 5. While this is occurring, charge neutralization develops allowing for flocculation, because the cationic sites attract anionic particles [1, 4]. The patch must be thicker than the electrostatic double layer in order for flocculation to occur [1]. Shear can break up the flocs produced by the patch mechanism but the fibers can reflocculate [17]. Cationic polymers of low molecular weight with a high charge density are the most useful for the patch mechanism [4].

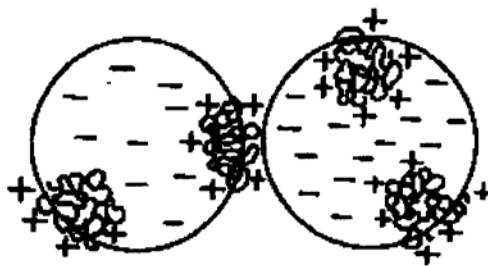


Figure 5: Patch mechanism [1].

2.5.4 Complex Flocculation

Complex flocculation consists of four different mechanisms which are dual polymer flocculation, microparticle flocculation, network flocculation, and site blocking flocculation [17]. A dual polymer flocculation mechanism consists of both a cationic polymer and an anionic polymer. First, the cationic polymer is added to solution to form positive sites on the fibers [4, 17]. Then, the anionic polymer is added to form bridges to the cationic sites on the fibers inducing flocculation [4, 17]. Microparticle flocculation uses a cationic polymer with an anionic particle that has a high surface area [4]. The cationic polymer uses a bridging mechanism after it is added to the solution to create fiber flocs [17]. These flocs are then broken up by applying shear forces and the anionic particles are added to reflocculate the fibers into stronger flocs [17]. Network flocculation is the third type of complex flocculation and involves the use of hydrogen bonds. During this mechanism, two polymers form a network which gathers colloidal particles as they travel through the liquid suspension [1]. The final mechanism is that of site blocking. Site blocking is used to decrease possible sites for polymer adsorption. Better polymer conformations are achieved by utilizing site blocking agents which improve bridging [17].

2.6 Flocculation Kinetics

Flocculation kinetics describe the rate at which fibers combine with one another or how other particles in the suspension attach to the fibers. According to Neimo, the kinetics are dependent on several factors such as bonding ability of the particulates and collision frequency of the contents in solution [17]. Understanding flocculation kinetics is important for the study of fines retention and retention of other colloids.

2.6.1 Techniques for Measuring Flocculation Kinetics

Several instruments can be used to study flocculation kinetics such as a light scattering technique, dynamic drainage jar, and more recently the use of a high-speed camera. The light scattering method does not allow for visualization of fiber flocs but the high-speed camera captures images that can be analyzed by software to measure floc characteristics. Light scattering uses a laser where the light is reflected by the solid particles [18]. A phototransistor accepts the scattered light and converts it to a frequency that can be analyzed [19]. This frequency power spectrum can be changed to a wavelength power spectrum and the size of the flocs can be determined given this information [19]. Advances in new technology promoted the use of high-speed cameras for data acquisition of flocculation behavior. The camera is capable of capturing images at high speeds and then the acquired images are converted to grey scale for analysis [20, 21]. Using the grey value of the images, the average concentration of the fibers can be determined [21]. A fast Fourier transform can be performed which can distinguish the flocculation behavior in different wave length ranges [21, 22]. Image analysis is capable of determining several pieces of information including: flocculation kinetics, floc area, floc diameter, and local concentration of fibers.

2.6.2 Reporting Flocculation Kinetics

Flocculation kinetics have previously been reported by the degree of flocculation also known as the floc index [19, 23]. In a solution, flocculation needs to be measured by a variable fiber distribution [24]. The degree of flocculation is a function of the fiber concentration and the variation of fiber concentration [22, 23]. The floc index accounts for the variation of floc size of before and after polymer addition [23]. According to

Wagberg and Eriksson, when using image analysis or light scattering techniques the degree of flocculation is calculated from the change in grey-values from before and after polymer addition [21]. Flocculation kinetics have also been previously reported with the use of rate constants such as a deposition and detachment rate constants which are both a function of fiber concentration [25].

2.6.3 Results of Flocculation Kinetics

Cationic polyacrylamide (cPAM) is a commonly used flocculating agent and results on flocculation kinetics and mechanisms are published in previous literature. According to Wagberg and Lindstrom, the flocculation index and floc diameter increase after polymer addition quickly and level off after 0.5 seconds [23]. Solberg and Wagberg show that after the flocculation index reaches a maximum it will decrease with increasing cPAM dosage [26]. Regarding fiber fines, when mixed in with fibers and cPAM the fines will floc to a maximum and then detach [27]. Asselman and Garnier report that fiber fines concentration will decrease after being mixed with polymer coated fibers, but after a few minutes will return to the initial concentration due to polymer transfer from coated fibers to fines [28].

CHAPTER 3

EXPERIMENTAL

3.1 Fiber and Polymer Preparation

The trials conducted consisted of determining the effect of varying fiber length on floc formation. The total fiber amount administered into the system equaled 0.04 grams fiber on a dry basis. The amount of water present in the sample equaled 500 mL. Experiments included trials of 2/3 long fiber with 1/3 short fiber, 1/3 long fiber with 2/3 short fiber, all long fiber, and unfractionated fiber.

3.1.1 Short and Long Fiber Separation

To obtain a large difference in fiber length between short and long fibers a Bauer-Mcnett classifier was used. Another option to achieve short fibers was to refine the fibers. Refining drastically changes the physical properties of the fibers, which made fractionating a more reasonable approach.

The standard TAPPI test method, T 233, was followed for use of the Bauer-McNett classifier. The process of fractionating required the use of 10 grams dry fiber. The pulp fiber must be disintegrated at 10,000 revolutions and then diluted with water to 2L. Screen sizes utilized were that of 10, 12, 35, and 60 mesh screens. The long fibers were a product of the 12 mesh screen and the short fibers were that of the 60 mesh screen. As a result of fractionation, the fines were removed since they can pass through a 60 mesh screen. The fibers were fractionated for 20 minutes in deionized water, and then the products collected from the bottom of the tanks on the classifier.

3.1.2 Fiber Quality Analyzer (FQA)

Fiber quality analysis (FQA) was carried out on the short and long fiber. In these experiments, FQA reported short and long fiber arithmetic mean lengths of 1.29 mm and 3.48 mm, respectively. FQA offered a comparison with the results obtained after image analysis. Figures of fiber length distribution are shown below.

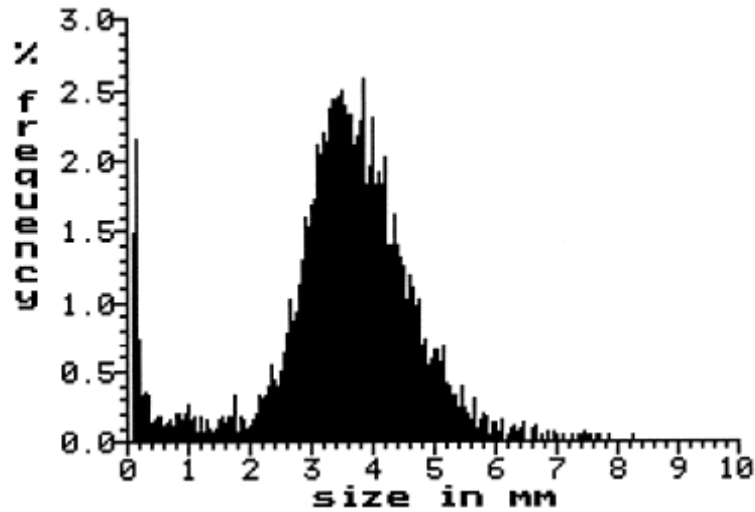


Figure 6: Long fiber length distribution (Screen size 12).

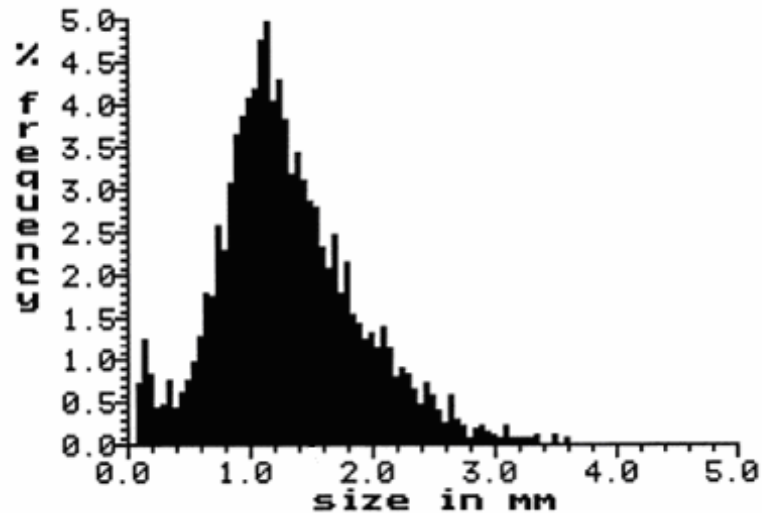


Figure 7: Short fiber length distribution (Screen size 60).

3.1.3 Cationic Polyacrylamide (cPAM) Preparation

The cPAM was supplied in the form of a powder, thus it needed to be dissolved in water for preparation. The amount of cPAM was 0.1 g powder per 100 mL of deionized water, which resulted in a concentration of 0.1%. Since the polymer can hydrolyze over time, it was prepared no more than one day before an experiment was conducted.

3.2 Procedure

The experiment required a total of 0.04 gm of fiber on a dry basis where the amounts of long and short fiber were varied depending on the trial. The experimental setup consisted of the camera, lens, 1000 mL beaker containing 500 mL deionized water, and the DC motor with the impeller attached as the stirring mechanism. The beaker containing the water was agitated by the impeller, and fiber was added to the beaker. The contents of the beaker resulted in a 0.01% consistency solution. The speed of the impeller was controlled by varying the voltage supplied to the DC motor and remained constant during a trial. The lighting had to be adjusted so that the background was black and the fibers appeared with a white coloration. Obtaining the proper lighting was done by changing the background behind the beaker, and the amount of light directed at the beaker. Once the lighting was correct, the 0.1% cPAM solution was injected into the beaker at the same time recording commenced. The video was recorded for 25 seconds capturing the flocculation process at 100 images per second. In order to analyze the images with Image J software, a length scale must be determined. To achieve a proper length scale a measuring device must be placed in the focal plane of the camera. Once the camera was focused on the measuring device then a screen shot was taken and used as a length scale in Image J. The video was analyzed and one image per second was studied over the course of 25 seconds, which resulted in 25 data points. In each image the

individual fibers that were not part of a floc were measured. An example of the images from the beginning, middle, and end can be seen in Figures 8, 9, and 10, respectively. These images are unfractionated fiber at 181 RPM with 2 ppm cPAM.

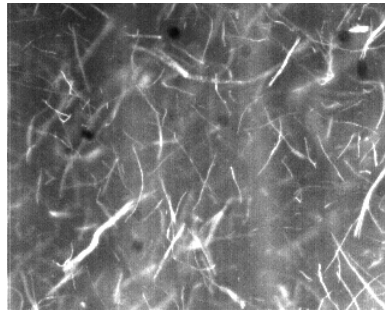


Figure 8: Beginning (Time = 0 sec).

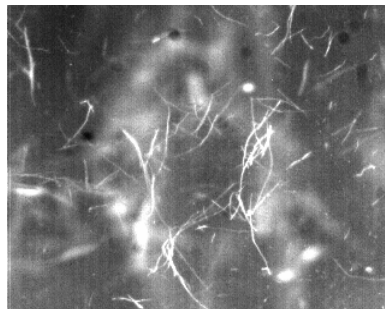


Figure 9: Middle (Time = 13 sec).

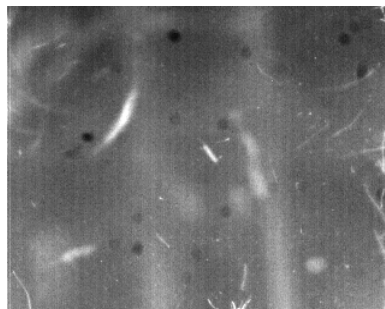


Figure 10: End (Time = 24 sec).

The average individual fiber length (fibers that were not part of a floc) was then plotted versus time. The depth of field of the camera was approximately 3.5 cm. In each image the individual fibers were counted and ranged from 30-60 fibers initially and 10-20 fibers after flocculation. This is shown in Table 1.

Table 1: Amount of fiber present at the beginning and conclusion of a trial at 181 RPM and 2 ppm cPAM.

Trial	Avg. Initial Amount of Fibers	Avg. Final Amount of Fibers
All Long Fiber	24	11
2/3 Long Fiber	35	18
1/3 Long Fiber	52	29
Unfractionated	35	13

The variables that can be controlled include the amount of cPAM added, speed of the impeller, and the quantity of different fiber lengths. Experiments that were carried out are shown in the Table 2.

Table 2: All of the trials performed.

Trial	Unfractionated Fiber Amount Dry Basis (gm)	Long Fiber Amount Dry Basis (gm)	Short Fiber Amount Dry Basis (gm)	cPAM Amount (ppm)	Motor Speed (RPM)
1	0	0.027	0.013	2	100
2	0	0.027	0.013	2	181
3	0	0.027	0.013	2	250
4	0	0.027	0.013	4	100
5	0	0.027	0.013	4	181
6	0	0.027	0.013	4	250
7	0	0.027	0.013	1	181
8	0	0.027	0.013	0.2	181
9	0	0.027	0.013	0.1	181
10	0	0.013	0.027	2	100
11	0	0.013	0.027	2	181
12	0	0.013	0.027	2	250
13	0	0.013	0.027	4	100
14	0	0.013	0.027	4	181
15	0	0.013	0.027	4	250
16	0	0.013	0.027	1	181
17	0	0.013	0.027	0.2	181
18	0	0.013	0.027	0.1	181
19	0	0.04	0	2	100
20	0	0.04	0	2	181
21	0	0.04	0	2	250
22	0	0.04	0	4	100
23	0	0.04	0	4	181
24	0	0.04	0	4	250
25	0	0.04	0	1	181
26	0	0.04	0	0.2	181
27	0	0.04	0	0.1	181
28	0.04	0	0	2	100
29	0.04	0	0	2	181
30	0.04	0	0	2	250
31	0.04	0	0	4	100
32	0.04	0	0	4	181
33	0.04	0	0	4	250
34	0.04	0	0	1	181
35	0.04	0	0	0.2	181
36	0.04	0	0	0.1	181

3.3 Measurement Error

The error incurred in this study is mostly due to human error during image analysis. Since the individual fibers are measured without the use of a particle analyzer, more error is present than if the software measured the data. Error is calculated by choosing 5 consecutive images that are each 0.01 seconds apart from one another. These images should have about the same average fiber length because they are taken on the scale of hundredths of a second. The error is reported as a relative standard deviation of 4.1%. Relative standard deviation is calculated simply by dividing the standard deviation by the arithmetic mean fiber length. Other sources of error could include amount of fiber added, volume of water, and amount of cPAM added. The error from these sources is not accounted for because they are significantly lower than that of image analysis.

3.4 Replication

Trials were repeated to confirm that the data could be replicated. The graph below, Figure 11, shows the trial of unfractionated fiber at 181 RPM and 2 ppm cPAM.

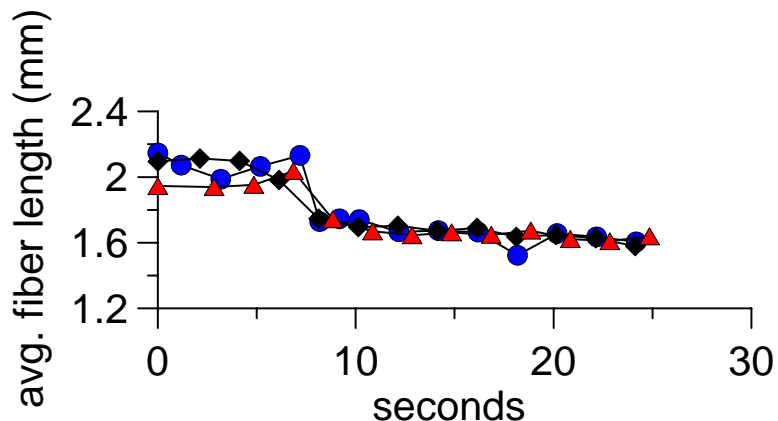


Figure 11: Graph of 3 trials of unfractionated fiber at 181 RPM and 2 ppm cPAM.

Inferring from Figure 11, all 3 trials proved to produce similar results. The average fiber length starts to decline at the same point and the ending fiber length is approximately identical. The next 3 figures show the replication of trials with 1/3 long, 2/3 long, and all long fiber, respectively.

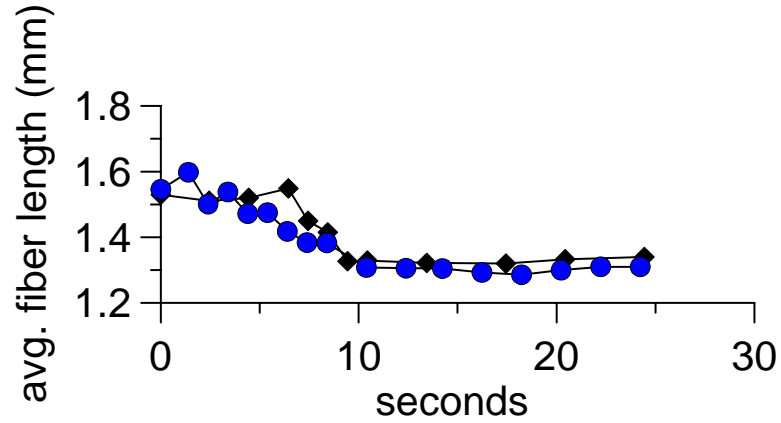


Figure 12: Graph of 1/3 long and 2/3 short fiber at 181 RPM and 2 ppm cPAM.

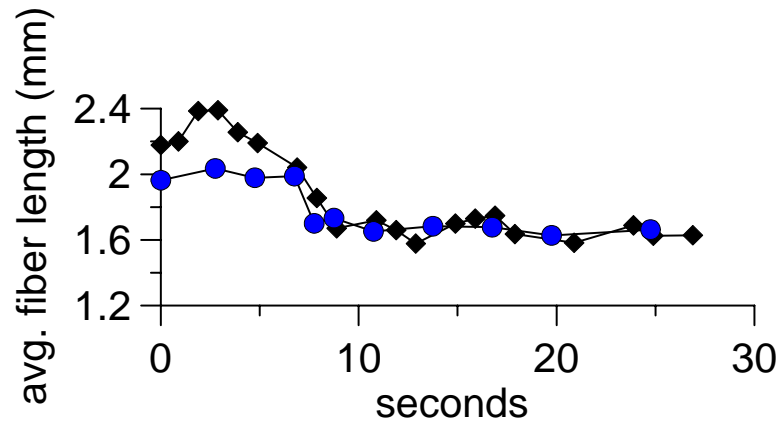


Figure 13: Graph of 2/3 long and 1/3 short fiber at 181 RPM and 2 ppm cPAM.

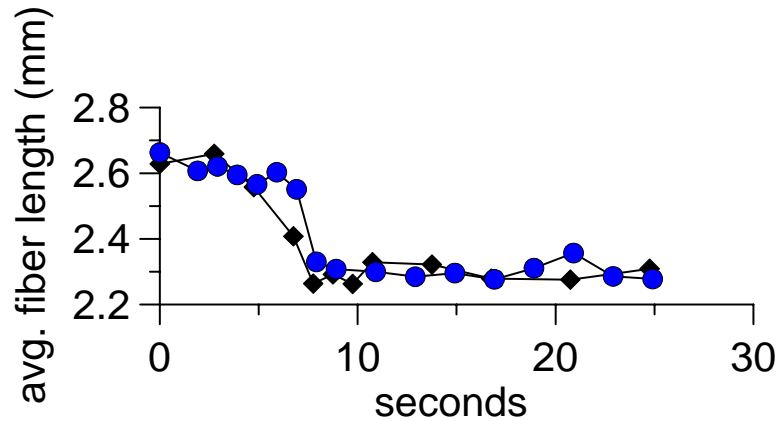


Figure 14: Graph of all long fiber at 181 RPM and 2 ppm cPAM.

3.5 Materials

- The pulp consists of virgin brown softwood fibers, freeness of 700 mL, and kappa number of 100. It was supplied by Inland's mill in Rome, Ga.
- The primary polymer was a cationic polyacrylamide (cPAM) provided by Hercules and was referenced as DI373.
- The secondary polymer was provided by Eka Chemical and is named Eka 2610. This polymer is a low charge, high molecular weight, cationic polyacrylamide.
- 1000 mL beaker with a diameter of 9 cm and height of 18.5 cm
- Pittman 24 volt DC miniature gear motor consisting of a 5.9:1 gear ratio.
- Voltage controller
- Impeller with a diameter of 4.5 cm
- Micro-Nikkor lens 105 mm f/2.8 made by Nikon
- Phantom v4.2 high-speed camera made by Vision Research
- Image J software provided by National Institutes of Health (NIH)

CHAPTER 4

RESULTS AND DISCUSSION

4.1 Long Fiber (2/3) and Short Fiber (1/3)

The initial trials performed used 2/3 long fiber and 1/3 short fiber. Since the total amount of fiber on a dry basis was 0.04 grams, this resulted in 0.027 grams long fiber and 0.013 grams short fiber on a dry basis. The fibers were then added to 500 mL of water, which provided a consistency of 0.01%. The parameters that were varied for these fiber lengths are listed in Table 3. The parameter “Fiber reduction %” is actually a quantity proportional to fiber reduction %, because the projection of the image results in undercounting of the fibers. The fiber reduction percentage is simply the percentage reduction of free fiber (not part of a floc) in solution from the start of the trial to the end of the trial. In this study this “quantity” will still be referred to as fiber reduction %. Also, when describing fiber length reduction, the physical properties of the fibers are not being altered. Fiber length reduction is not the physical cutting or shortening of fibers, but is simply the reduction of individual average fiber length due to longer fibers getting trapped in fiber flocs and shorter fibers left in solution.

Table 3: Different trials performed for 2/3 long and 1/3 short fiber.

Trial	Unfractionated Fiber Amount Dry Basis (gm)	Long Fiber Amount Dry Basis (gm)	Short Fiber Amount Dry Basis (gm)	cPAM Amount (ppm)	Motor Speed (RPM)	Fiber redu- ction %
1	0	0.027	0.013	2	100	45
2	0	0.027	0.013	2	181	46.5
3	0	0.027	0.013	2	250	30.5
4	0	0.027	0.013	4	100	40
5	0	0.027	0.013	4	181	33
6	0	0.027	0.013	4	250	28.8
7	0	0.027	0.013	1	181	44
8	0	0.027	0.013	0.2	181	43.5
9	0	0.027	0.013	0.1	181	39

Graphs were prepared from the results of each trial to make a comparison of the collected data. Figure 15 represents the different motor speeds at a constant cPAM concentration of 2 ppm.

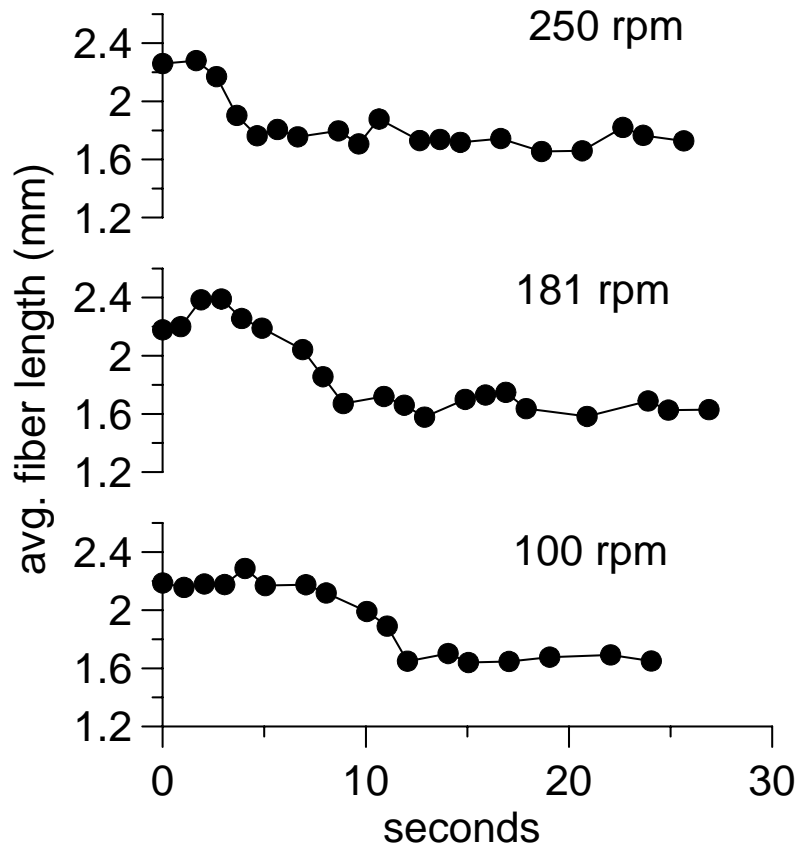


Figure 15: Graph of 2/3 long and 1/3 short fiber, 2 ppm cPAM, and varying motor speeds of 100 RPM, 181 RPM, and 250 RPM.

In Figure 15, the y-axis represents the average fiber length that was not part of a fiber floc. The results of Figure 15 show that the individual fiber length decreased with time but eventually leveled off. The motor speed played a role in fiber length reduction, as increasing the speed of the motor resulted in faster flocculation and a more rapid decrease in fiber length. A higher shear rate allowed the polymer to disperse in the solution more quickly. Since the polymer dispersed faster, this affected the flocculation rate making it faster as well. To account for the decreased fiber length, shorter fibers float in and out of the flocs but were not retained in the floc structure like the larger fibers.

Figure 16 represents the results of 3 different motor speeds, while holding the cPAM concentration constant at 4 ppm.

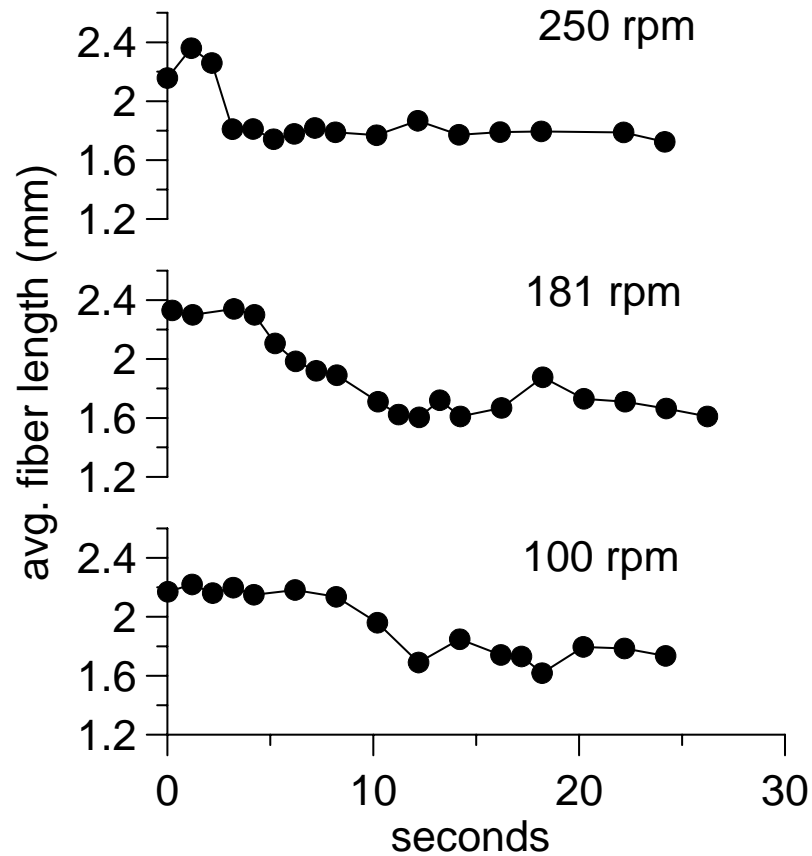


Figure 16: Graph of 2/3 long and 1/3 short fiber, 4 ppm cPAM, and varying motor speeds of 100 RPM, 181 RPM, and 250 RPM.

The increased concentration of cPAM to 4 ppm produced the same trend as that of 2 ppm. The fiber length noticeably decreased with time and more quickly at higher shear rates. At 250 RPM the fiber length decreased to 1.68 mm within 3 seconds, at 181 RPM after 6 seconds, and at 100 RPM around 10 seconds.

The increase in cPAM concentration from 2 ppm to 4 ppm did not have a noticeable impact on flocculation because cPAM is positively charged and attached to the

negative sites on the fibers. Thus, the open negative sites on the fibers were attracted to the positive polymer sites inducing flocculation. A maximum was reached, where doubling the concentration of the cPAM had no effect because the available sites had been consumed.

The following figure further displays the effect of cPAM concentration on fiber length and flocculation rate.

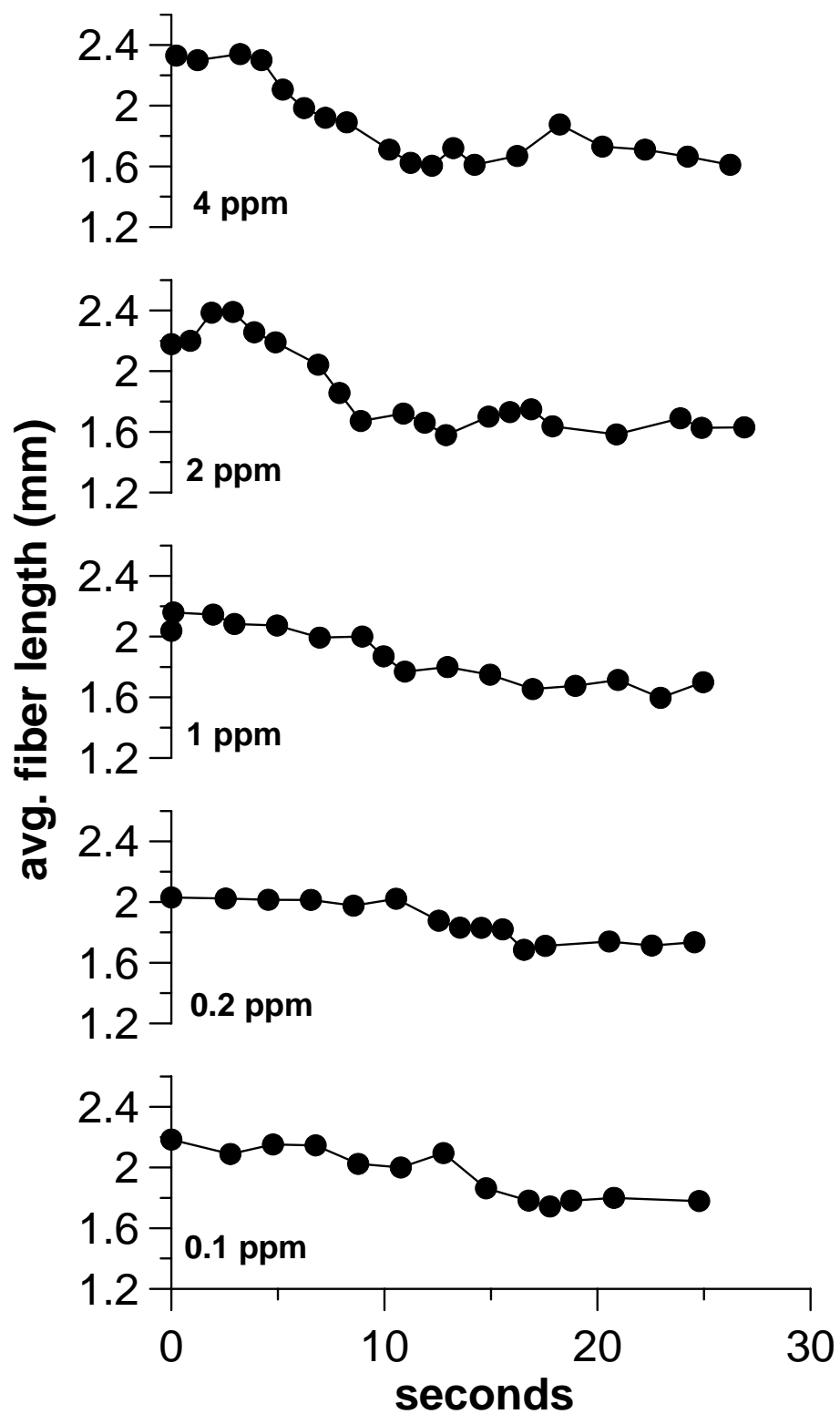


Figure 17: Graph of 2/3 long fiber at cPAM concentrations of 0.1, 0.2, 1, 2, and 4 ppm at a motor speed of 181 RPM.

In Figure 17 the average fiber length is affected by cPAM concentration. The greater the amount of cPAM the more the fiber length decreases. However, at an increased concentration above 2 ppm the cPAM adsorption reaches a maximum because fiber length no longer decreases. Also, with an increase in concentration the average fiber length sees a quicker decay compared to results of lower concentrations. Table 4 shows the average length of the remaining individual fibers before and after flocculation.

Table 4: The starting and final avg. fiber lengths as a function of polymer concentration.

cPAM Concentration (ppm)	Starting Avg. Fiber Length (mm)	Final Avg. Fiber Length (mm)
0.1	2.10	1.78
0.2	2.01	1.72
1	2.07	1.67
2	2.23	1.63
4	2.27	1.68

From the table it is noticeable that with higher cPAM addition the final average fiber length reduces.

4.2 Long fiber (1/3) and Short fiber (2/3)

In the next set of trials performed, the long fiber amount was decreased while the short fibers were increased. The total amount of fiber remained the same at 0.04 grams on a dry basis. This amount was an equivalent of 0.027 grams short fiber and 0.013 grams of long fiber on a dry basis. The fibers were then added to 500 mL of water, resulting in a consistency of 0.01%. The different trials completed are shown below in Table 5.

Table 5: Different trials performed for 1/3 long and 2/3 short fiber.

Trial	Unfractionated Fiber Amount Dry Basis (gm)	Long Fiber Amount Dry Basis (gm)	Short Fiber Amount Dry Basis (gm)	cPAM Amount (ppm)	Motor Speed (RPM)	Fiber redu- ction %
10	0	0.013	0.027	2	100	43.1
11	0	0.013	0.027	2	181	46.8
12	0	0.013	0.027	2	250	54
13	0	0.013	0.027	4	100	33.1
14	0	0.013	0.027	4	181	37.5
15	0	0.013	0.027	4	250	41.7
16	0	0.013	0.027	1	181	42.2
17	0	0.013	0.027	0.2	181	27.3
18	0	0.013	0.027	0.1	181	44.8

The first graph shows the results of 3 different motor speeds while holding the cPAM concentration constant at 2 ppm in Figure 18.

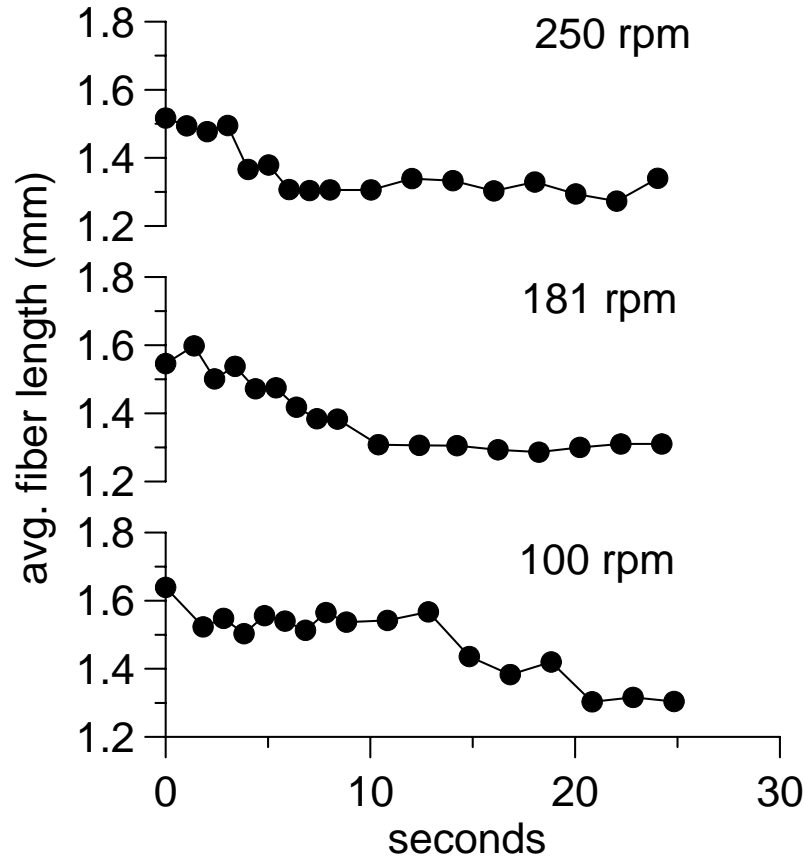


Figure 18: Graph of 1/3 long and 2/3 short fiber, 2 ppm cPAM, and varying motor speeds of 100 RPM, 181 RPM, and 250 RPM.

The figure above shows a decline in average fiber length with time. As before, the speed played an important role in the flocculation rate. Increased shear rate lead to better mixing and scattering of the polymer. The polymer adsorbed to the fiber surface more quickly at high RPM's, resulting in a rapid reduction of fiber length. The average fiber length began lower than the trials of 2/3 long and 1/3 short because there was less long fiber present in the study. Floccing takes longer here than in Figure 15. The number of fibers per unit volume in Figure 18 will be higher than that of Figure 15 because the same mass of pulp was used but there are more fibers present in the short fiber samples.

The next figure, Figure 19, represents the results of 3 different motor speeds, while holding the cPAM concentration constant at 4 ppm.

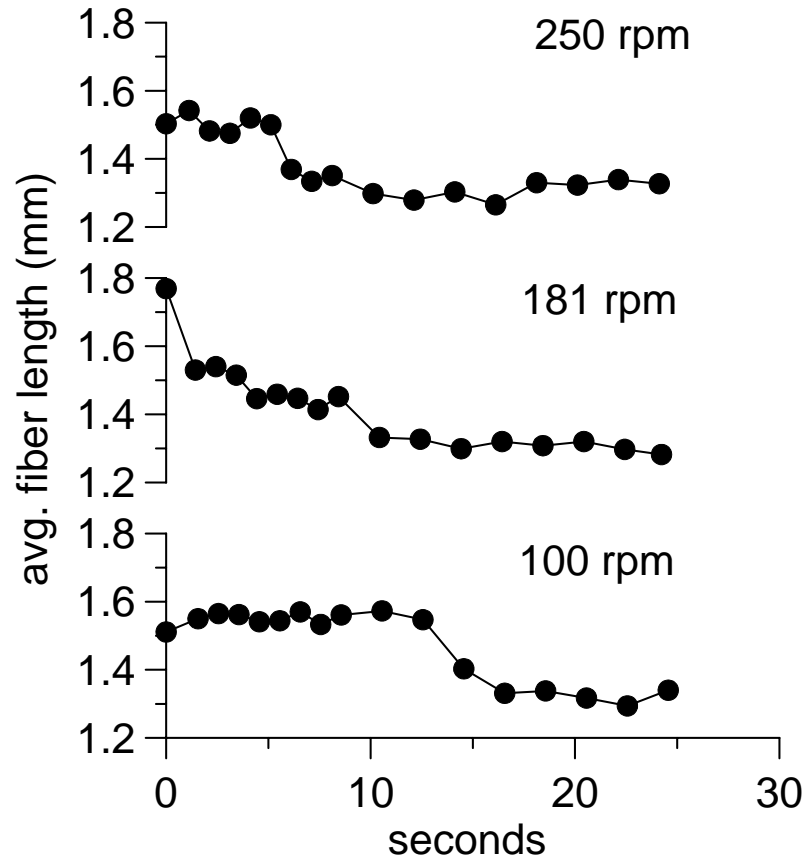


Figure 19: Graph of 1/3 long and 2/3 short fiber, 4 ppm cPAM, and varying motor speeds of 100 RPM, 181 RPM, and 250 RPM.

In the above figure, the line representing 181 RPM declines rapidly. To explain this result, the cPAM may have been added slightly before recording initiated, which contributed to a faster decrease in fiber length than the previous graphs. It was previously concluded that the increased cPAM concentration does not have a corresponding effect on flocculation rate. Thus, an error may have been made prior to recording or during image analysis.

The results from this data demonstrate that the polymer concentration has no significant impact on fiber length reduction after 2 ppm. The key factor in the rate of flocculation was the motor speed. These results are similar to those of 2/3 long and 1/3 short fiber.

Trials were conducted at various cPAM additions at a constant motor speed of 181 RPM and this can be seen in Figure 20.

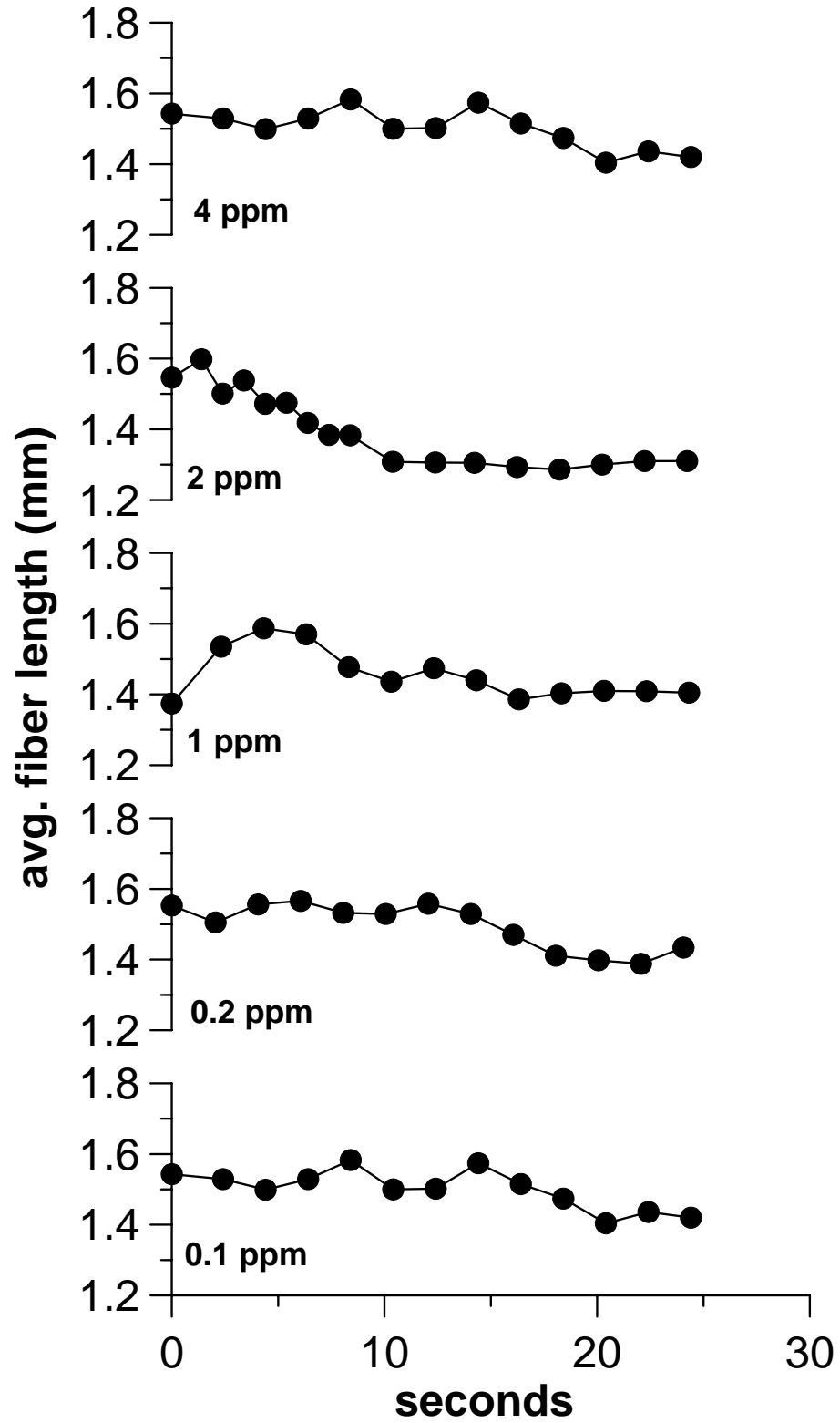


Figure 20: Graph of 1/3 long fiber at cPAM concentrations of 0.1, 0.2, 1, 2, and 4 ppm at a motor speed of 181 RPM.

The effects of cPAM concentration are not as noticeable in this figure. The table below is a better representation of the average fiber length.

Table 6: The starting and final avg. fiber lengths as a function of polymer concentration.

cPAM Concentration (ppm)	Starting Avg. Fiber Length (mm)	Final Avg. Fiber Length (mm)
0.1	1.53	1.42
0.2	1.54	1.41
1	1.52	1.40
2	1.55	1.30
4	1.59	1.30

From the table one can infer that the increasing concentration of cPAM results in a further decay of fiber length.

4.3 All Long Fiber

The next set of trials performed contained of all long fiber. The fiber amount totaled 0.04 grams on a dry basis. The fiber was added to 500 mL of water composing a solution of 0.01% consistency. Table 7 shows the variations of cPAM and motor speed with each experiment.

Table 7: Different trials performed for all long fiber.

Trial	Unfractionated Fiber Amount Dry Basis (gm)	Long Fiber Amount Dry Basis (gm)	Short Fiber Amount Dry Basis (gm)	cPAM Amount (ppm)	Motor Speed (RPM)	Fiber redu- ction %
19	0	0.04	0	2	100	64
20	0	0.04	0	2	181	55.3
21	0	0.04	0	2	250	33
22	0	0.04	0	4	100	43
23	0	0.04	0	4	181	59.5
24	0	0.04	0	4	250	35
25	0	0.04	0	1	181	60
26	0	0.04	0	0.2	181	45
27	0	0.04	0	0.1	181	51

The first graph shows the results of 3 different motor speeds, while holding the cPAM concentration constant at 2 ppm in Figure 21.

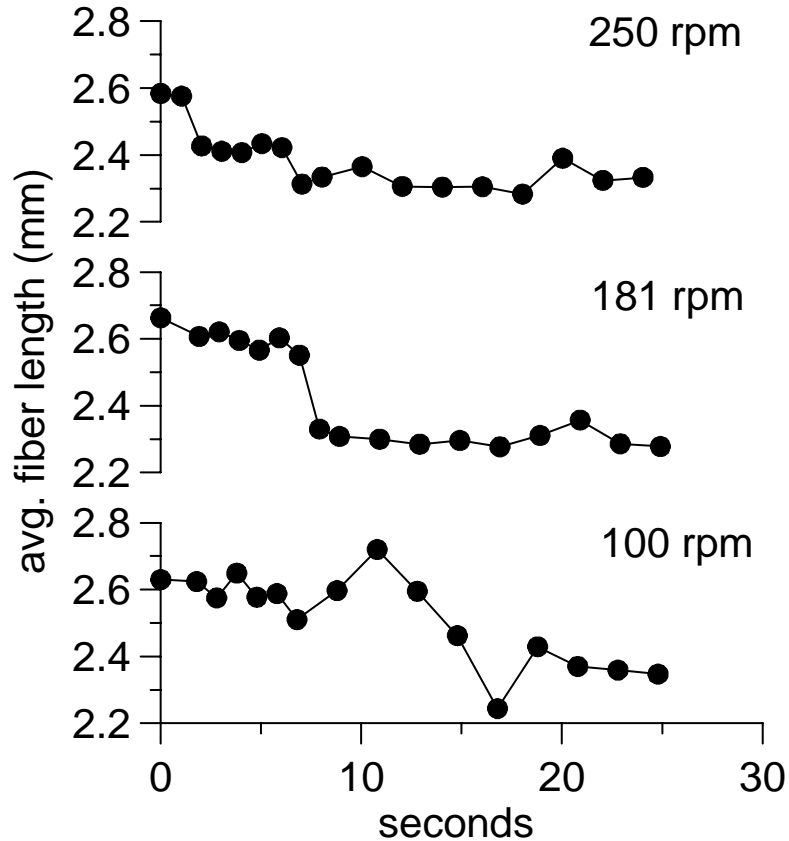


Figure 21: Graph of all long fiber, 2 ppm cPAM, and varying motor speeds of 100 RPM, 181 RPM, and 250 RPM.

The average fiber length is noticeably higher than that of the other trials conducted because there was not any short fiber added. The fiber length demonstrates a reduction over time; if there were only long fibers present, there should not have been a decrease in fiber length. However, there still existed short fibers in the sample, since fractionating does not remove every short fiber. Short fibers still get caught in the 12 mesh screen in the Bauer McNett classifier depending on their orientation when approaching the screen. Additionally, the short fibers attach to long fibers already in contact with the screen, preventing them from passing through. Evidently, enough short fibers were trapped on the screen to have an impact and appear in the graphs. The

average starting fiber length for this experiment was about 2.6 mm, while FQA reported an arithmetic mean length of 3.48 mm. There are a few reasons for disagreement of average fiber length. First, FQA measured thousands of fibers, whereas image analysis only measured approximately 40 fibers per image. Counting more fibers is a better representation of the system as a whole. Second, when using image analysis the camera only was focused on one plane of view. If a fiber was in a different focal plane, then its measurement was slightly off. Since there are many fibers measured outside of this plane, this resulted in error during image analysis.

Figure 22 represents the results of 3 different motor speeds, while holding the cPAM concentration constant at 4 ppm.

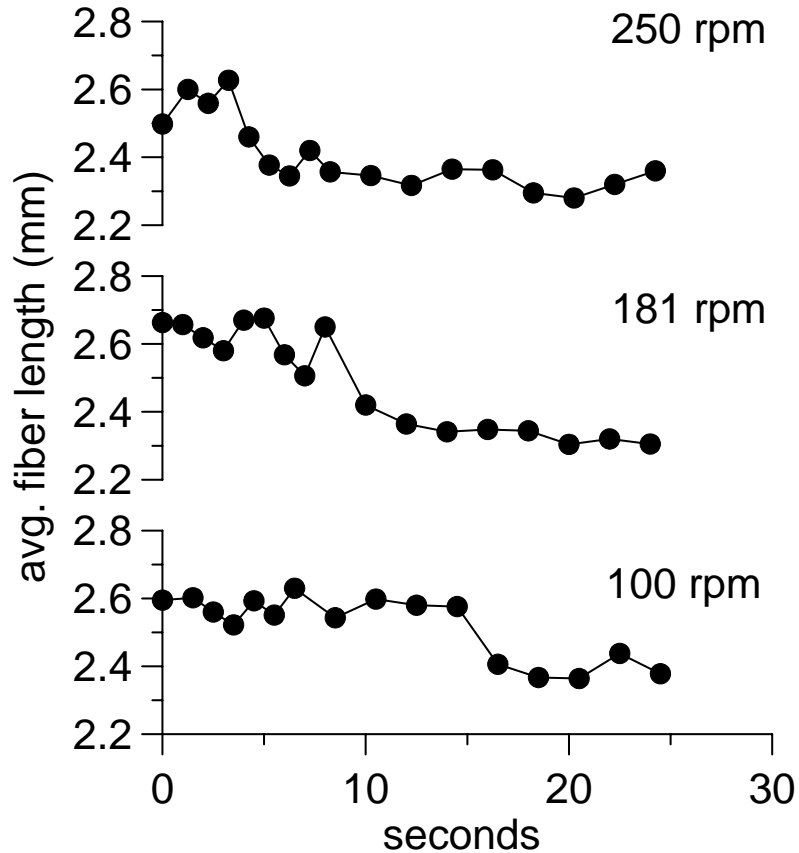


Figure 22: Graph of all long fiber, 4 ppm cPAM, and varying motor speeds of 100 RPM, 181 RPM, and 250 RPM.

Increasing cPAM concentration after 2 ppm has no effect on the flocculation rate of long fiber similar to the other fiber length variations.

From the previous graphs one can infer that the cPAM concentration once again does not have a significant enough impact over 2 ppm on flocculation to be accounted for. The motor speed is the most important when dealing with flocculation kinetics. This effect can also be seen in the figure below.

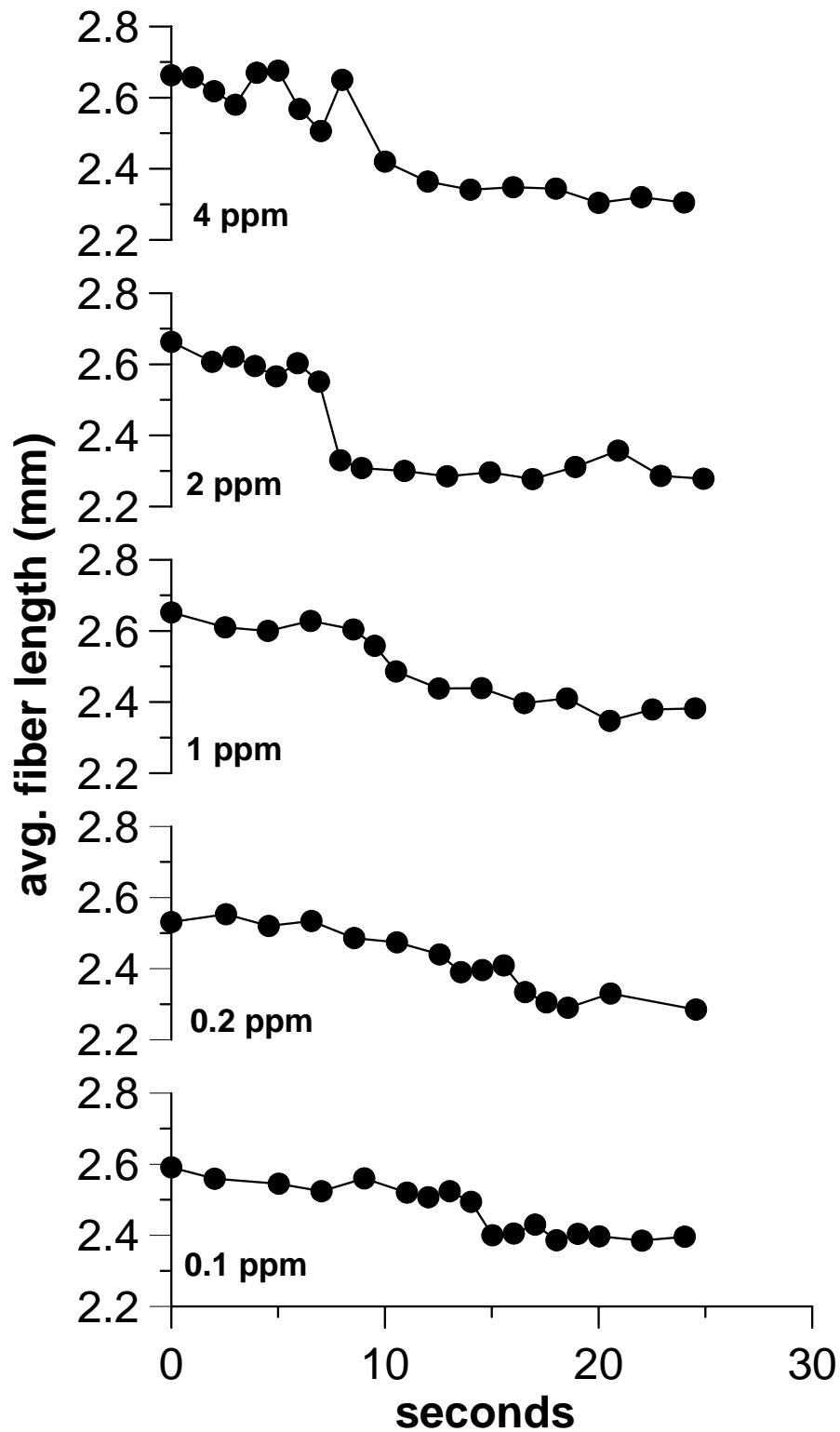


Figure 23: Graph of all long fiber at cPAM concentrations of 0.1, 0.2, 1, 2, and 4 ppm at a motor speed of 181 RPM.

From the graph, with a greater dosage of cPAM the fiber length reduces more quickly and to a further extent. This is also quantified in the table below.

Table 8: The starting and final avg. fiber lengths as a function of polymer concentration.

cPAM Concentration (ppm)	Starting Avg. Fiber Length (mm)	Final Avg. Fiber Length (mm)
0.1	2.54	2.40
0.2	2.54	2.37
1	2.61	2.38
2	2.60	2.30
4	2.62	2.32

The table shows that the fiber length decreases with an increase in cPAM concentration. The effect is most noticeable at the 2 ppm addition. Prior to 2 ppm the other concentrations have a minimal result on the decline of fiber length.

4.4 Unfractionated Fiber

The final set of trials consisted of the original unfractionated pulp. On a dry basis the fiber weight was that of 0.04 gm. After fiber addition to 500 mL of water the resulting consistency of the solution was 0.01%. The table below lists the different experiments performed.

Table 9: Different trials performed for unfractionated fiber.

Trial	Unfractionated Fiber Amount Dry Basis (gm)	Long Fiber Amount Dry Basis (gm)	Short Fiber Amount Dry Basis (gm)	cPAM Amount (ppm)	Motor Speed (RPM)	Fiber redu- ction %
28	0.04	0	0	2	100	68.3
29	0.04	0	0	2	181	60.4
30	0.04	0	0	2	250	71.3
31	0.04	0	0	4	100	51.2
32	0.04	0	0	4	181	65.5
33	0.04	0	0	4	250	55.9
34	0.04	0	0	1	181	76.5
35	0.04	0	0	0.2	181	60.9
36	0.04	0	0	0.1	181	2.4

The first graph shows the results of 3 different motor speeds, while holding the cPAM concentration constant at 2 ppm in Figure 24.

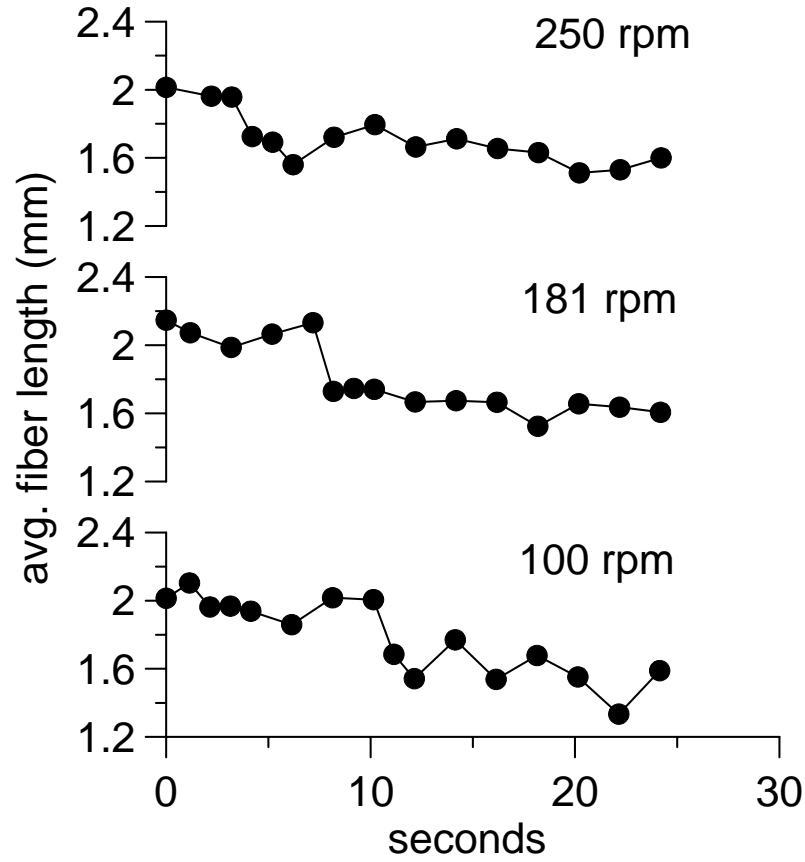


Figure 24: Graph of unfractionated fiber, 2 ppm cPAM, and varying motor speeds of 100 RPM, 181 RPM, and 250 RPM.

By observing this figure it is noticeable that the fiber length decreases with time just as that of the other trials with different fiber length. Also, the higher the RPM the faster the decay of fiber length. Unfractionated fiber has the same results as that of other fiber lengths.

The next figure, Figure 25, shows the results of motor speed and a cPAM concentration of 4 ppm.

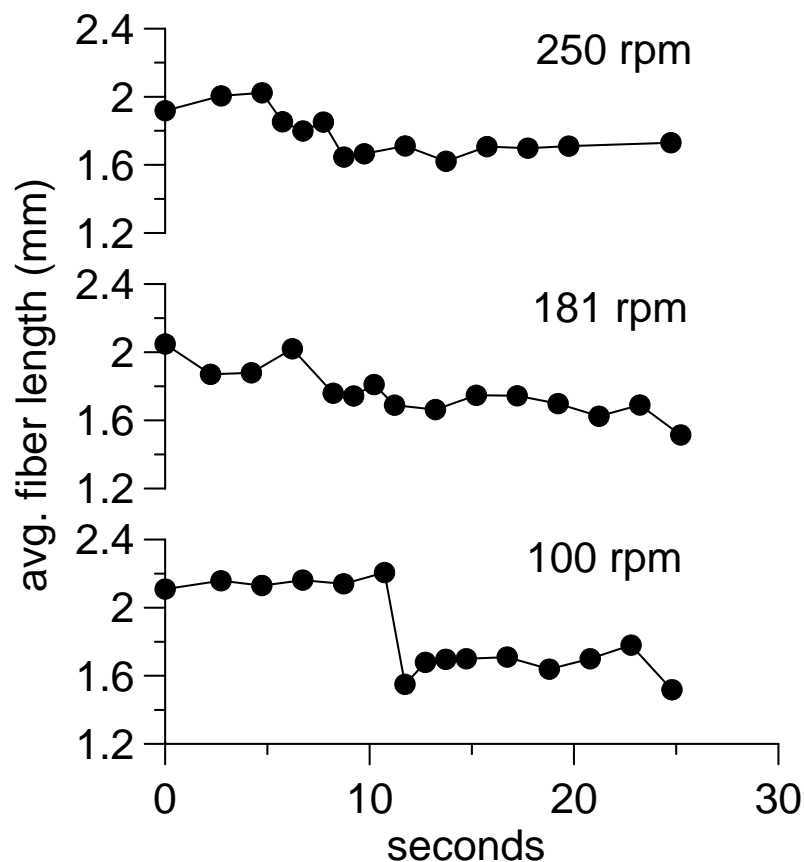


Figure 25: Graph of unfractionated fiber, 4 ppm cPAM, and varying motor speeds of 100 RPM, 181 RPM, and 250 RPM.

After increasing the polymer concentration to 4 ppm the results are similar to that of the 2 ppm trials. Comparing this to the other fiber lengths the results are similar.

The next graph, Figure 26, displays the effect of varying cPAM concentration at a constant motor speed. The different concentrations experimented include 0.1, 0.2, 1, 2, and 4 ppm.

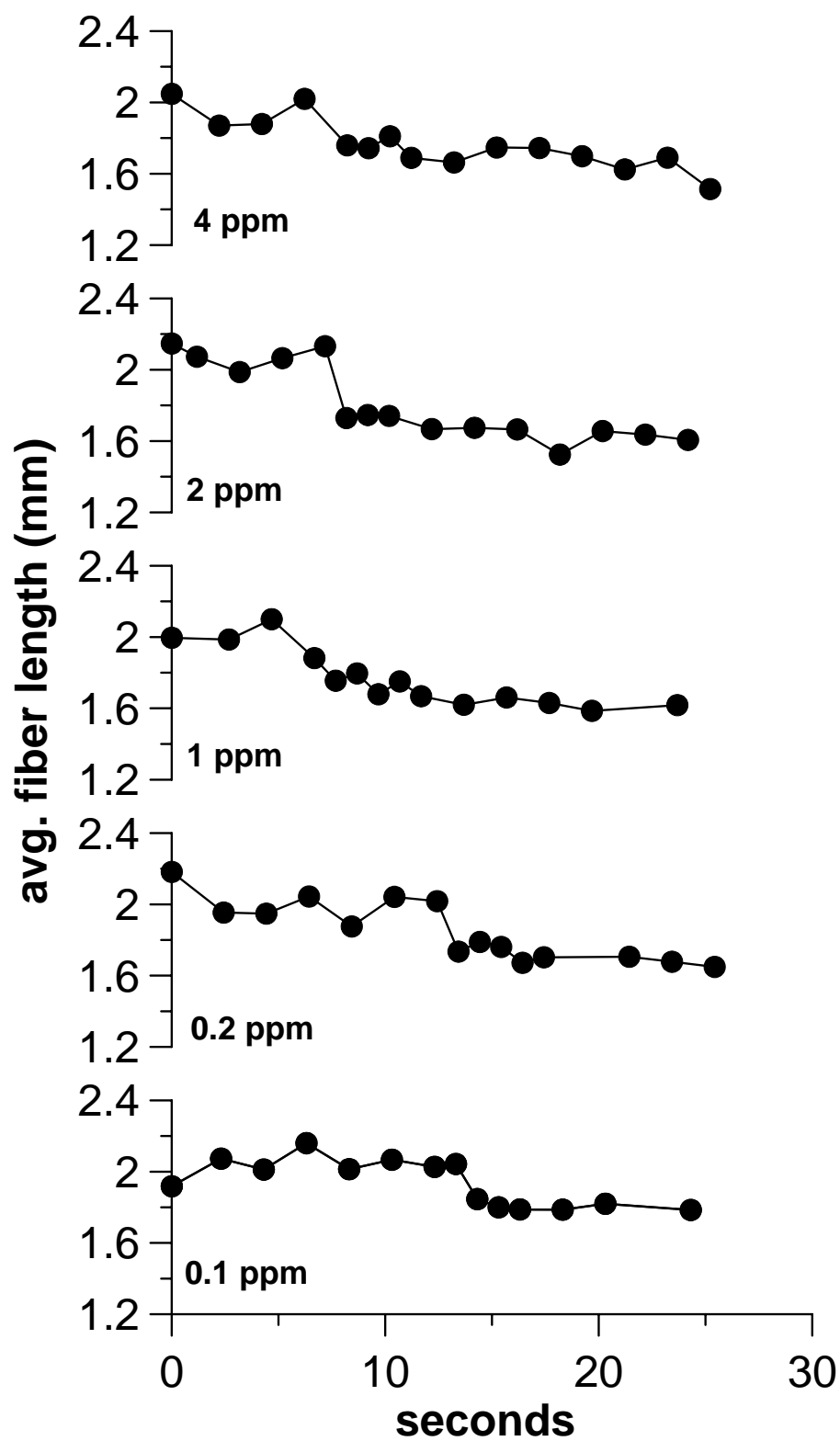


Figure 26: Graph of unfractionated fiber at cPAM concentrations of 0.1, 0.2, 1, 2, and 4 ppm at a motor speed of 181 RPM.

By observing the trends from this graph, one might notice the final average fiber length at decreased concentrations of cPAM is longer than that of increased concentrations. The table below lists the final fiber lengths of the respective trials.

Table 10: The starting and final avg. fiber lengths as a function of polymer concentration.

cPAM Concentration (ppm)	Starting Avg. Fiber Length (mm)	Final Avg. Fiber Length (mm)
0.1	2.04	1.80
0.2	2.01	1.68
1	2.03	1.63
2	2.08	1.64
4	2.04	1.63

This table shows that at a low concentration of 0.1 ppm the polymer has a minimal effect on fiber length decay compared to that of the increased dosages. After an addition of 1 ppm of polymer the effect is the same thus negating the need for more than 1 ppm.

4.5 Comparison of Different Fiber Amounts

All of the data is plotted to provide a cumulative comparison of the results. In Figures 27, 28, and 29 that data is displayed for 100 RPM, 181 RPM, and 250 RPM, respectively. The cPAM concentration is that of 2 ppm.

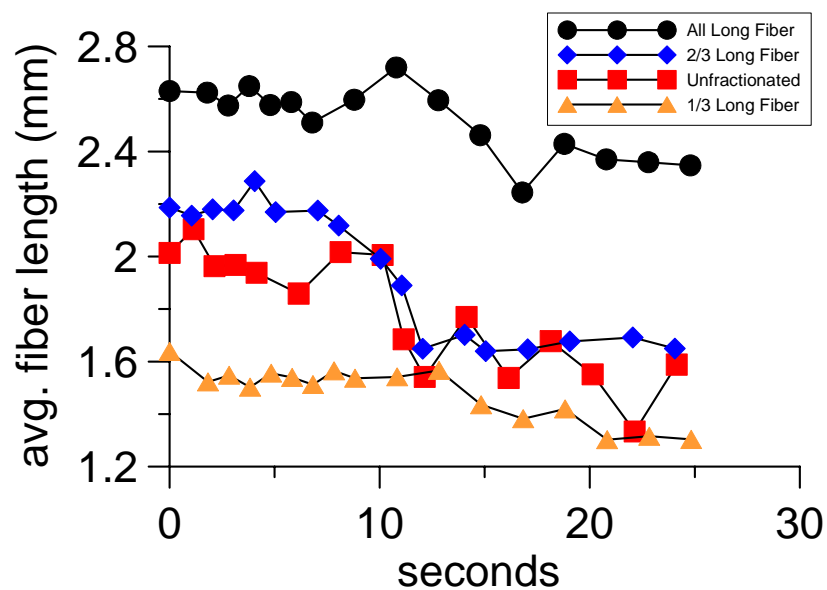


Figure 27: Graph of all long fiber, 2/3 long with 1/3 short, 1/3 long with 2/3 short, 100 RPM, and a cPAM concentration of 2 ppm.

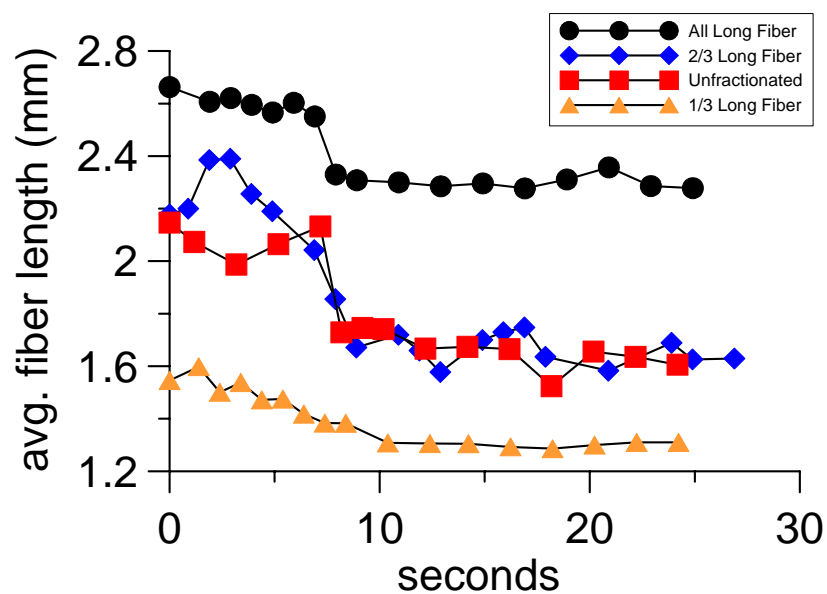


Figure 28: Graph of all long fiber, 2/3 long with 1/3 short, 1/3 long with 2/3 short, 181 RPM, and a cPAM concentration of 2 ppm.

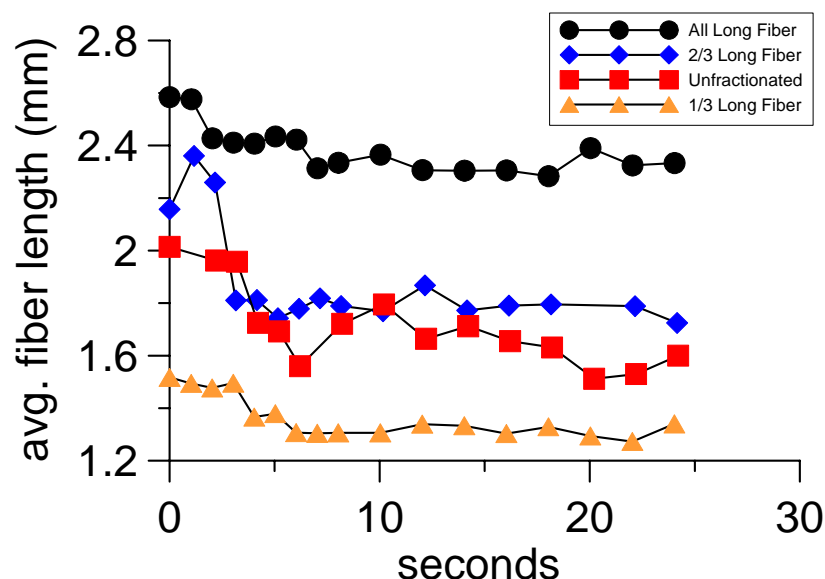


Figure 29: Graph of all long fiber, 2/3 long with 1/3 short, 1/3 long with 2/3 short, 250 RPM, and a cPAM concentration of 2 ppm.

Inferring from Figures 27, 28, and 29 it is noticed that the 2/3 long with 1/3 short fiber combination has a steeper middle slope than that of the other fiber combinations. From this a conclusion is made that a more rapid flocculation rate occurs with the 2/3 long and 1/3 short mixture. This result may just be coincidental because there is quite a bit of error involved with image analysis. The slopes and fiber length reduction of the 1/3 long with 2/3 short fiber and all long fiber are relatively the same. The time at which flocculation begins is close when comparing 1/3 long with 2/3 short fiber to the trend line of all long fiber.

4.6 cPAM Isotherm

An isotherm was constructed at 181 RPM and the various concentrations of polymer with unfractionated fiber. The isotherm displays the point at which additional polymer dosage will not increase flocculation or effect fiber length.

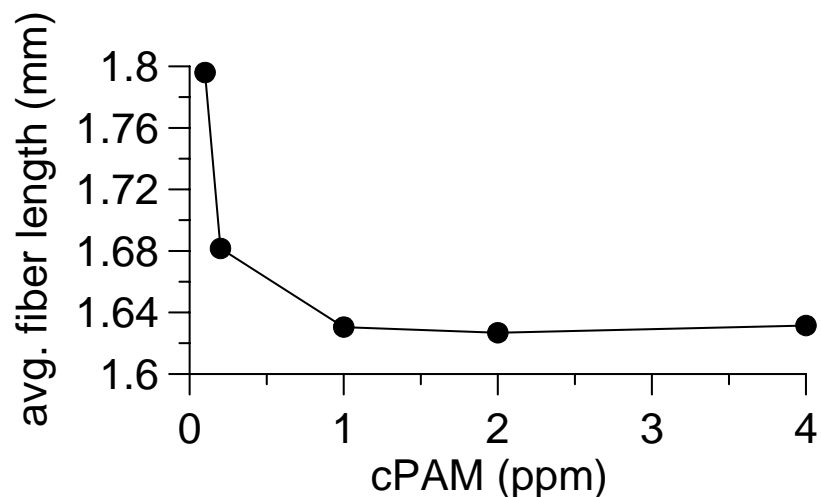


Figure 30: cPAM isotherm at 181 RPM and various concentrations of polymer.

Figure 30 shows that after a concentration of 1 ppm the increased polymer dosage has the same effect. Also, at a low addition of 0.1 ppm the polymer proves to have a minimal effect on fiber length reduction.

4.7 Effects of a Different Polymer

A different polymer was supplied to offer a contrast to the polymer that was tested. The additional polymer is cPAM with low charge and high molecular weight. Eka is the supplier and the trade name of the polymer is Eka 2610. A comparison can be made by interpreting the graph below of unfractionated fiber, 2 ppm, and 181 RPM.

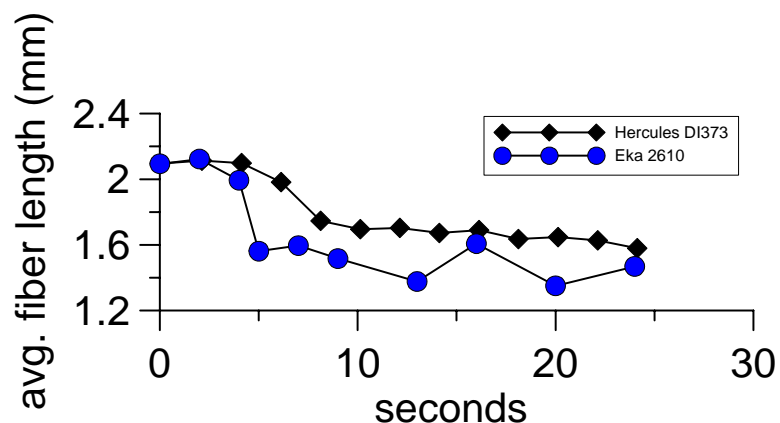


Figure 31: Graph of unfractionated fiber at 181 rpm and 2 ppm of Hercules DI373 and Eka 2610.

Figure 31 shows that the Eka polymer produced results more rapidly than that of Hercules DI373. This may be due to the difference in charge and molecular weight.

Table 11: Comparison of results for the Eka and Hercules polymers.

cPAM Version	Charge	Molecular Weight	Starting Avg. Fiber Length (mm)	Final Avg. Fiber Length (mm)	Fiber reduction %
Hercules DI373	Low	High	2.08	1.61	60
Eka 2610	Low	High	2.07	1.46	83

4.8 Effects of Shear Rate

Shear rate played impacted flocculation and the reduction of fiber length. Trials were performed at speeds higher than that of 250 RPM; however, they are not reported here because flocculation did not occur. Having too high of shear rate prevented fiber flocs from forming, thus there was not a decrease in fiber length. Additionally, experiments were conducted below 100 RPM, and these values were not reported as well. The camera contained enough memory to hold a 30 second video clip, and below 100 RPM the time required for fibers to floc was greater than 30 seconds. This time constraint did not offer enough data points to make a comparative graph. Reynolds

numbers were calculated, based on the diameter of the impeller, at each RPM and are as follows: $Re_{100 \text{ RPM}} = 3792$, $Re_{181 \text{ RPM}} = 6863$, and $Re_{250 \text{ RPM}} = 9480$. Reynolds numbers between 2000 and 3000 were avoided because this is between the regimes of laminar and turbulent flow. Experiments conducted below 100 RPM were either between laminar and turbulent flow or consisted of complete laminar flow. If the flow was not turbulent then this resulted in insufficient mixing. At Reynolds numbers above 10,000 the flow was too turbulent preventing floc formation.

4.9 Fiber Length

Trials were performed consisting of all short fibers, but the results were inconclusive. The fibers resulted in flocs; however, the fiber length did not decrease with time. The resulting fiber flocs of all short fibers were smaller than those trials containing long fiber. The fiber length distribution with the small fibers was not as great as that of the large fibers, which explains not having a significant decrease in fiber length. When using the Bauer McNett classifier, the size 60 screen was implemented to capture the short fibers. Smaller fibers were able to pass through the screen, and larger fibers already retained by the other screens resulted in a tight distribution of fiber length. The fiber length distribution of short fibers, provided by FQA, was between 0.5 mm and 2.0 mm, whereas the large fiber distribution had a greater range of 2.0 mm to 5.0 mm. This explains why all long fiber was able to be used in a trial and all short fiber had more difficulty producing relevant results.

The average fiber length produced by the camera was less than that of FQA. This occurred because of the way FQA measures fiber length and the focal plane of the camera. The camera was only focused on one plane of view resulting in fiber measurements being shorter due to a number of fibers out of focus. Using FQA, some of

the fiber curls get straightened out in the machine before measurement. Fiber curl in image analysis does not get straightened out producing a shorter average fiber length compared to FQA results. Also, when measuring fibers via image analysis, some fibers were at an angle resulting in a shorter measurement. This occurred because the fibers were being imaged from a side view. To account for this, a new average fiber length was calculated at angles from 0° to 90° based on an original fiber length and then the ratio was taken. For example, the original fiber length was the hypotenuse of a right triangle and held constant while solving for the adjacent side using angles from 0° to 90° . The ratio of new fiber length to original fiber length equaled 0.64. This means that using image analysis the fiber length was about 64% of the actual fiber length. The ratio of image analysis fiber length to FQA fiber length was 0.74. The value of 0.64 is relatively close to 0.74 meaning that since some of the fibers were at an angle during measurement this could explain why the value of FQA does not match that of image analysis.

Figure 32 displays the decrease in fractional fiber length with cPAM concentration. This graph was constructed to demonstrate the relationship between the decrease in fiber length with cPAM concentration.

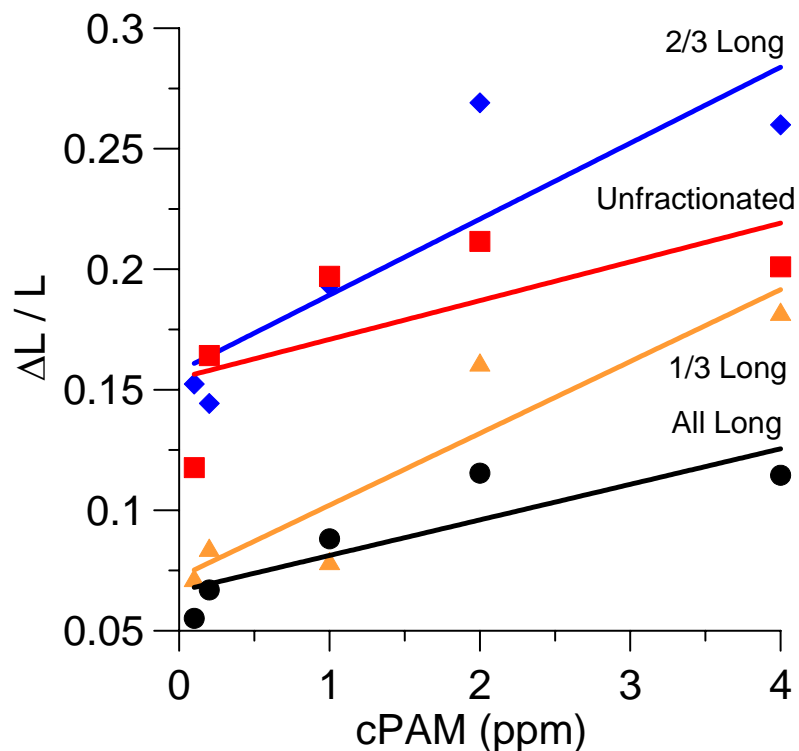


Figure 32: Difference in final and initial average fiber lengths with varying concentrations of cPAM.

4.10 Fiber Floc Characterization

There are several ways to characterize fiber floc information such as light scattering, which uses a laser beam to measure particle size. High-speed cameras can also be used, which provide digital videos and images. These images can be analyzed using ImageJ software provided by National Institutes of Health (NIH). Fibers are easily counted and measured using the software. The images are extracted from a 25 second video clip, which allows sufficient time for the fibers to floc after the polymer addition.

CHAPTER 5

CONCLUSIONS/SUMMARY

This study quantifies what happens to the fiber length before and after polymer addition. Different experiments were conducted varying the amount of short and long fibers added as well as polymer concentration. Motor speed also played an important role in the rate of fiber length reduction.

The results of changing the motor speed displayed that at higher RPM's the polymer could be mixed more quickly and fiber length reduction occurred faster than at a lower RPM. Also, if the speed was too high then this caused floc breakup.

Polymer concentration affected the reduction in fiber length. The outcome of 2 and 4 ppm were nearly the same due to a plateau in length reduction. Once the concentration dropped below 1 ppm the fiber length did not reduce as significantly as the higher concentrated experiments. Comparing the Hercules and Eka polymers, the Eka polymer had quicker fiber length reduction and the fiber length decreased slightly more than that of the Hercules polymer.

Fiber length reduction was noticeable in all trials conducted. Also, the amount of free fiber decreased as flocculation occurred. This study showed that flocculation consists of chemical and mechanical processes. For a given fiber mixture the average fiber length drops about 20%. A key finding is that no further drop occurs regardless of motor speed or cPAM concentration. Fiber flocs of a given size, which are dictated by the initial fiber mixture, can only trap fibers above a given size and smaller fibers will not

be collected. Table 12 shows the conclusions of starting fiber length and final fiber length.

Table 12: Starting average fiber length and final average fiber length.

Fiber	Motor Speed (RPM)	cPAM Concentration (ppm)	Starting Avg. Fiber Length (mm)	Final Avg. Fiber Length (mm)
Long Fiber (2/3) and Short Fiber (1/3)	181	0.1	2.10	1.78
	181	0.2	2.01	1.72
	181	1	2.07	1.67
	181	2	2.23	1.63
	181	4	2.27	1.68
Long fiber (1/3) and Short fiber (2/3)	181	0.1	1.53	1.42
	181	0.2	1.54	1.41
	181	1	1.52	1.40
	181	2	1.55	1.30
	181	4	1.59	1.30
All Long Fiber	181	0.1	2.54	2.40
	181	0.2	2.54	2.37
	181	1	2.61	2.38
	181	2	2.60	2.30
	181	4	2.62	2.32
Unfractionated Fiber	181	0.1	2.04	1.80
	181	0.2	2.01	1.68
	181	1	2.03	1.63
	181	2	2.08	1.64
	181	4	1.95	1.63

This study occurs in solution and does not produce the same results as a Britt Jar experiment or actual paper machine. When employing a Britt Jar, the fibers measured are fibers not part of a floc, but some of the smaller fibers are retained on the screen or filtered out by the flocs. With the example of a paper machine, when the fibers and fillers hit the wire some of the smaller particles will pass through. However, as the sheet builds up most of the fines and fillers will be retained in the sheet, thus removing the

smaller particles from solution. If all of the fibers are left in solution this provides a more accurate approach to measuring the decrease in fiber length.

High-speed imaging proved to be a useful tool in acquiring and analyzing images. Fiber length reduction during flocculation was able to be quantified with the use of a high-speed camera.

REFERENCES

- [1] Eklund, D. and T. Lindstrom, *Paper Chemistry: An Introduction*. 1991: DT Paper Science Publications.
- [2] Smook, G.A., *Handbook for Pulp and Paper Technologists*. 2nd ed. 1992: Angus Wilde.
- [3] Niskanen, K., *Paper Physics*. Papermaking Science and Technology. 1998: Fapet Oy.
- [4] Scott, W.E., *Principals of Wet End Chemistry*. 1996: TAPPI Press.
- [5] Britt, K.W. and J.E. Unbehend, *New methods for monitoring retention*. TAPPI, 1976. **59**(2): p. 67-70.
- [6] Htun, M. and A. De Ruvo, *The implication of the fines fraction for the properties of bleached kraft sheets*. Svensk Papperstidning, 1978. **81**(16): p. 507-510.
- [7] Marton, J., *The role of surface chemistry in fines - cationic starch interactions*. TAPPI, 1980. **63**(4): p. 87-91.
- [8] Mason, S.G., *The flocculation of pulp suspensions and the formation of paper*. TAPPI, 1950. **33**(9): p. 440-444.
- [9] Takeuchi, N., et al., *Formation and destruction of fiber flocs in a flowing pulp suspension*. Appita, 1983. **37**(3): p. 223-230.
- [10] Beghello, L. and D. Eklund, *Some mechanisms that govern fiber flocculation*. Nordic Pulp and Paper Research Journal, 1997. **12**(2): p. 119-123.
- [11] Kerekes, R.J. and C.J. Schell, *Characterization of Fiber Flocculation Regimes by a Crowding Factor*. Journal of Pulp and Paper Science, 1992. **18**(1): p. J32-J38.
- [12] Runkana, V., P. Somasundaran, and P.C. Kapur, *A population balance model for flocculation of colloidal suspensions by polymer bridging*. Chemical Engineering Science, 2006. **61**(1): p. 182-191.
- [13] Chen, B., D. Tatsumi, and T. Matsumoto, *Floc structure and flow properties of pulp fiber suspensions*. Journal of the Society of Rheology, Japan, 2002. **30**(1): p. 19-25.

- [14] Kerekes, R.J., R.M. Soszynski, and P.A. Tam Doo, *The Flocculation of Pulp Fibres*, in *Papermaking Raw Materials in Transactions of the 8th Fundamental Research Symposium Held at Oxford, September, 1985*. 1985. p. 265-306.
- [15] Yan, H., T. Lindstrom, and M. Christiernin, *Some ways to decrease fibre suspension flocculation and improve sheet formation*. Nordic Pulp and Paper Research Journal, 2006. **21**(1): p. 36-43.
- [16] Unbehend, J.E., *Mechanisms of "soft" and "hard" floc formation in dynamic retention measurement*. TAPPI, 1976. **59**(10): p. 74-77.
- [17] Neimo, L., *Papermaking Chemistry*. Papermaking Science and Technology. 1999: Fapet Oy.
- [18] Gruber, E. and P. Muller, *Investigations of the flocculation behavior of microparticle retention systems*, in *TAPPI Papermakers Conference*. 2006. p. 293-306.
- [19] Wagberg, L., *A device for measuring the kinetics of flocculation following polymer addition in turbulent fiber suspension*. Svensk Papperstidning, 1985. **88**(6): p. R48-R56.
- [20] Beghello, L., et al. *Device for measuring fiber floc sizes in highly turbulent fiber suspensions*. in *International Paper Physics Conference*. 1995.
- [21] Wagberg, L. and J. Eriksson, *New equipment for detection of polymer induced flocculation of cellulosic fibres by using image analysis - application to microparticle systems*. Chemical Engineering Journal, 2000. **80**(1-3): p. 51-63.
- [22] Wagberg, L. and T. Nordqvist, *Detection of polymer induced flocculation of cellulosic fibres by image analysis*. Nordic Pulp and Paper Research Journal, 1999. **14**(3): p. 247-255.
- [23] Wagberg, L. and T. Lindstrom, *Kinetics of polymer-induced flocculation of cellulosic fibers in turbulent flow*. Colloids and Surfaces, 1987. **27**(1-3): p. 29-42.
- [24] Wahren, D., *Proposed definitions of some basic papermaking terms*. Svensk Papperstidning, 1967. **70**(21): p. 725-729.
- [25] Asselman, T. and G. Garnier, *Mechanism of Polyelectrolyte Transfer during Heteroflocculation*. Langmuir, 2000. **16**(11): p. 4871-4876.
- [26] Solberg, D. and L. Wagberg, *On the mechanism of cationic-polyacrylamide-induced flocculation and re-dispersion of a pulp fiber dispersion*. Nordic Pulp and Paper Research Journal, 2003. **18**(1): p. 51-55.

- [27] Van de Ven, T.G.M., M.A. Qasaimeh, and J. Paris, *Fines Deposition on Pulp Fibers and Fines Flocculation in a Turbulent-Flow Loop*. Industrial and Engineering Chemistry Research, 2005. **44**(5): p. 1291-1295.
- [28] Asselman, T. and G. Garnier, *Polymer transfer during fines detachment under turbulent flow: mechanism and implications*. Journal of Pulp and Paper Science, 2001. **27**(2): p. 60-65.